17. Kharasch ED, Whittington D, Hoffer C. Influence of hepatic and intestinal cytochrome P4503A activity on the acute disposition and effects of oral transmucosal fentanyl citrate. *Anesthesiology*. 2004;101:729–737.
18. Tegeder I, Lötsch J, Geisslinger G. Pharmacokinetics of opioids in liver disease. *Clin Pharmacokinet*. 1999;37: 17–40.
19. Zhang W, Chang YZ, Kan QC, et al. CYP3A4*1G genetic polymorphism influences CYP3A activity and response to fentanyl in Chinese gynecologic patients. *Eur J Clin Pharmacol*. 2010;66:61–66.
20. Otis J, Rothman M. A phase III study to assess the clinical utility of low-dose fentanyl transdermal system in patients with chronic nonmalignant pain. *Curr Med Res Opin*. 2006;22: 1493–1501.
21. Thompson JP, Bower S, Liddle AM, et al. Perioperative pharmacokinetics of transdermal fentanyl in elderly and young adult patients. *Br J Anaesth*. 1998;81:152–154.
22. Gupta SK, Hwang S, Southam M, et al. Effects of application site and subject demographics on the pharmacokinetics of fentanyl HCl patient-controlled transdermal system (PCTS). *Clin Pharmacokinet*. 2005;44:25–32.
23. Björkman S, Stanski DR, Verotta D, et al. Comparative tissue concentration profiles of fentanyl and alfentanil in humans predicted from tissue/blood partition data obtained in rats. *Anesthesiology*. 1990;72:865–873.

Journal of Neurochemistry

JOURNAL OF NEUROCHEMISTRY | 2011 | 118 | 256–265 doi: 10.1111/j.1471-4159.2011.07297.x

ORIGINAL ARTICLE

Pre-emptive morphine treatment abolishes nerve injury-induced lysophospholipid synthesis in mass spectrometrical analysis

Jun Nagai and Hiroshi Ueda

Division of Molecular Pharmacology and Neuroscience, Nagasaki University Graduate School of Biomedical Sciences, Nagasaki, Japan

Abstract

We have previously demonstrated that lysophosphatidic acid (LPA) production in the spinal cord following partial sciatic nerve injury (SCNI) and its signaling initiate neuropathic pain. In order to examine whether LPA production depends on the intense nociceptive signal, we have attempted to see suppression by pre-emptive treatment with centrally administered morphine, which mainly inhibits nociceptive signal at the level of spinal cord. In the present study, we developed a quantitative mass spectrometry assay to simultaneously analyze several species of lysophosphatidyl choline (LPC). The levels of 16:0-, 18:0- and 18:1-LPC in the spinal cord and dorsal root were maximally increased at 75 min after SCNI and then declined, as LPC is converted to LPA by autotaxin (ATX). In *atx*$^{+/-}$-mice, on the other hand, these levels were similar to wild-type mice at 75 min, but maximal at 120 min, suggesting that this difference is partly due to the low conversion of LPC to LPA in *atx*$^{+/-}$-mice. When morphine was centrally administered before SCNI, the injury-induced increase of LPC was completely abolished. These results suggest that LPC (or LPA) is produced by injury-induced nociceptive signal, which is effectively and pre-emptively suppressed by central morphine, possibly through known descending anti-nociceptive pathways.

Keywords: autotaxin, lysophosphatidyl choline, mass spectrometry, morphine, neuropathic pain, pre-emptive analgesia.

J. Neurochem. (2011) **118**, 256–265.

Lysophosphatidic acid (LPA) plays various physiological or pathophysiological roles as one of lipid mediators (Noguchi *et al.* 2009; Choi *et al.* 2010; Chun *et al.* 2010; Lin *et al.* 2010; Ueda 2011). This lipid mediator is synthesized in biological fluids including blood from lysophosphatidylcholine (LPC) by autotaxin (ATX), possessing lysophospholipase D activity (Tokumura 2002; Aoki *et al.* 2008). Although significant amounts of ATX are also present in the CSF, the levels of LPC and LPA are very low, suggesting that extracellular LPC production would be a rate-limiting step for LPA production (Nakamura *et al.* 2009). Recently, we have demonstrated that LPA is produced in the spinal cord (SC) (Ma *et al.* 2010b) and its LPA_1 receptor signaling initiates neuropathic pain and underlying mechanisms including demyelination in the dorsal root (DR), $Ca_v\alpha2\delta1$ up-regulation in the dorsal root ganglion (DRG) and protein kinase Cγ in the spinal cord, all which are supposed to contribute to neuropathic allodynia and hyperalgesia (Inoue *et al.* 2004; Ueda 2006, 2008, 2011). As the antagonistic blockade of LPA_1 receptor for 2–3 h after the injury abolished successive long-lasting abnormal pain (Ma *et al.* 2009a), LPA production is supposed to initiate neuropathic pain. Thus, we have currently focused on the LPA production in *in vitro* and *in vivo* studies (Inoue *et al.* 2008b; Ma *et al.*

Received January 23, 2011; revised manuscript received April 29, 2011; accepted May 2, 2011.

Address correspondence and reprint requests to Hiroshi Ueda, Division of Molecular Pharmacology and Neuroscience, Nagasaki University Graduate School of Biomedical Sciences, 1-14 Bunkyo-machi, Nagasaki 852-8521, Japan. E-mail: ueda@nagasaki-u.ac.jp

Abbreviations used: ATX, autotaxin; *atx*$^{+/-}$, mice heterozygous for *atx* gene; DR, dorsal root; DRG, dorsal root ganglion; LPA, lysophosphatidic acid; LPC, lysophosphatidyl choline; NALDI-TOF-MS, nanostructure-assisted laser desorption/ionization time-of-flight mass spectrometry; PLA_2, phospholipase A2; SC, spinal cord; SCNI, partial sciatic nerve injury; WT, wild-type.

2010a; b). In these studies, LPA levels have been measured as cell-rounding activities in B103 cells expressing LPA_1 receptor. LPA levels are increased only in the ipsilateral side of the dorsal half of SC and DR after partial sciatic nerve injury (SCNI), and the peak effects were observed at 3 h (Ma *et al.* 2010b). As ATX is largely lost in the *in vitro* studies using spinal cord slices, we have added recombinant ATX in the incubation medium and measured LPA, which had been converted from LPC. The elevation of LPA levels in spinal cord slices was reproduced only by the combination of different types of pain transmission by substance P and NMDA as an intense nociceptive model (Inoue *et al.* 2008b). Thus, it is hypothesized that the production of LPA, an initiator of neuropathic pain may occur by intense nociceptive signal to SC.

It is accepted that morphine exerts potent analgesia by driving descending anti-nociceptive system from midbrain periaqueductal gray matter or rostroventromedial medulla to spinal dorsal horn (Sato and Takagi 1971; Basbaum and Fields 1979; Fields *et al.* 2006). Based on the view that neuropathic pain is formed by a kind of memory-processes (Zhuo 2007), we have successfully demonstrated that the central pre-treatment with morphine to prevent the intense nociceptive input abolished long-lasting neuropathic pain (Rashid and Ueda 2005). This finding may provide the important evidence to support the existence of pre-emptive analgesia (Richmond *et al.* 1993). In the present study, we report the simultaneous quantitation method for multiple species of LPC by use of nanostructure-assisted laser desorption/ionization time-of-flight mass spectrometry (NALDI-TOF-MS) system and demonstrate the evidence for the prevention of LPC (as the LPA precursor) production by pre-emptive morphine treatment.

Materials and methods

Animals

Male mutant mice for the *atx* gene ($atx^{+/-}$) mice (Tanaka *et al.* 2006) and their sibling wild-type (WT) mice from the same genetic background (C57BL/6J), weighing 20–24 g, were used. They were housed at room temperature (21 ± 2°C) with free access to a standard laboratory diet and tap water. The procedures were approved by the Nagasaki University Animal Care Committee and complied with the recommendations of the International Association for the Study of Pain (Zimmermann 1983).

Partial ligation of sciatic nerve

Partial ligation of the sciatic nerve was performed under pentobarbital (50 mg/kg) anesthesia, according to the methods of Malmberg and Basbaum (1998). Briefly, the common sciatic nerve of the right hind limb was exposed at high thigh level through a small incision and the dorsal half of the nerve thickness was tightly ligated with a silk suture. A sham-operation was performed similarly except without touching the sciatic nerve.

Extraction of LPC from tissues

The unilateral dorsal half including dorsal horn (laminae I–V) of the lumber (L4–L6) spinal cord (SC) and L4–L6 DRs on the ipsilateral or contralateral side were then removed to enable the extraction of LPC as reported previously (Ma *et al.* 2009a; b). The averaged wet weights of the isolated unilateral SC and DRs in each mouse were 8 and 4 mg tissue weight, respectively. LPC were extracted from tissues according to modified methods (Sutphen *et al.* 2004). After their isolation, the tissue sample was placed in 1.5-mL tubes and homogenized by sonication in 250 μL of phosphate-buffered saline for approximately 30 s. The homogenates were then mixed with 1 mL of methanol/chloroform (2 : 1) and 30 μL of 10 N HCl were added in a glass tube (13 × 100 mm IWAKI). The samples were vortexed for 1 min and incubated on ice for 10 min. Chloroform (0.5 mL) and water (0.5 mL) were added for the formation of the two-phase system of the Bligh and Dyer method in acidic conditions (Bligh and Dyer 1959). The mixture was centrifuged at 2000 *g* for 10 min, and the chloroform phase was collected, and the remaining water/methanol phase was mixed with 0.5 mL of chloroform for another extraction. Subsequently, the chloroform phases were combined, dried with N_2 gas. The final sample was dissolved in as less as 50 μl of methanol and stored at −80 °C until use for analysis.

Nanostructure-assisted laser desorption/ionization time-of-flight mass spectrometry analyses

One microliter from 50 μL of finally obtained methanol solution was diluted with methanol (DR: 200–400 μL, SC: 400–600 μL) to adjust the concentration to the standard curve levels. One microliter of the sample including internal standard deuterium-labeled stearoyl (18:0)-LPC (D35-LPC) in a dose of 0.1 pmol (Doosan Serdary Research Laboratories, London, Canada) was spotted on the NALDI plate (Bruker Daltonics, Inc., Billerica, MA, USA). After drying, the sample was applied to an UltraflexI™ TOF/TOF systems (Bruker Daltonics, Inc.). Mass spectrometry was performed in the reflector mode, using an accelerating voltage of 25 kV. The laser energy was used at energy of 10–20% (1.0–2.0 μJ) and a repetition rate of 10 Hz. The mass spectra were calibrated externally using PEG 600 (Nacalai Tesque, Kyoto, Japan) as a standard peptide calibration. Each spectrum was produced by accumulating data from 300–500 consecutive laser shots. Standards of LPC were purchased from Sigma Chemical (St Louis, MO, USA) for 16:0-, 18:0- and 18:1-LPC, from Doosan Serdary Research Laboratories (London, Canada) for 18:2-, 18:3- and 20:4-LPC.

Identification of lysophosphatidyl choline species

In MS/MS analysis, mass spectra were acquired in LIFT mode using an UltraflexIII™ TOF/TOF systems (Bruker Daltonics, Inc.). The laser was used from 40% (4.0 μJ) to 60% (6.0 μJ). The mass spectra were obtained from ipsilateral spinal dorsal horn after nerve injury. Structure determination of lipid molecules was performed using lipid databases, such as LIPID MAPS (http://www.lipidmaps.org/) and the Lipid Search (http://lipidsearch.jp/), according to previous reports (Hsu and Turk 2003; Pulfer and Murphy 2003; Koizumi *et al.* 2010).

Statistical analysis

The differences between multiple groups were analyzed by one-way ANOVA with Tukey's multiple comparison *post hoc* analysis (Figs 5

and 7). The criterion of significance was set at $*p < 0.05$. All results are expressed as the mean ± SEM.

Results

Standard curve of lysophosphatidyl choline species by NALDI-TOF-MS

The NALDI plate is layered with nano-structured coating, which serves as an active matrix-free surface for desorption/ionization of spotted samples. The NALDI technique is optimal for the analysis of small molecules, such as LPC, because of low background (Wyatt *et al.* 2010). Typical charts of mass spectra with authentic standard reagents, 16:0-, 18:0-, 18:1-LPC, and internal standard D35-LPC at the level of 0.1 pmol/well were shown (Fig. 1a and c). However, the dose-related linearity of the ratios of ion-peak heights with each standard (16:0-, 18:0-, 18:1-, 18.2-, 18:3- and 20:4-LPC) at 0.01–1.0 pmol/well to the one with fixed D35-LPC (0.1 pmol/well) were shown (Fig. 1d and i). In this analysis, the signal derived from authentic species of LPC molecules was calculated by subtracting the basal background. The equation for linearity of 16:0-, 18:0-, 18:1-, 18:2-, 18:3- and 20:4-LPC levels were $y = 1441.5x$ ($R^2 = 0.982$), $y = 439.0x$ ($R^2 = 0.986$), $y = 922.3x$ ($R^2 = 0.976$), $y = 194.1x$ ($R^2 = 0.949$), $y = 1913.9x$ ($R^2 = 0.986$) and $y = 922.6x$ ($R^2 = 0.989$), respectively. The detection efficiency of 18:2-LPC was much lower than the others, although it remains what causes the difference.

Recovery yields of authentic LPC species

To examine the recovery yield of LPC through extraction and partial purification processes, 2 nmol of authentic 16:0-, 18:0- and 18:1-LPC were added to the tissue homogenates. Purified materials (in 50 μL methanol solution) were diluted by 400-fold volume of methanol, and 1 μL was plotted to the NALDI-TOF-MS plate (Fig. 2a and b). However, 0.1 pmol each of standard LPC mixture was analyzed as a control (Fig. 2c). When the LPC level was evaluated after adjusting to a standard curve, the recovery yield of LPC species was 70.6 ± 5.3% ($n = 4$) for 16:0-LPC, 85.1 ± 2.1% ($n = 4$) for 18:0-LPC and 89.6 ± 6.2% ($n = 4$) for 18:1-LPC, respectively.

Nerve injury-induced increase in the levels of LPC species in the spinal cord

The unilateral dorsal horn of the lumber spinal cord was isolated at 75 min after the partial injury of right sciatic

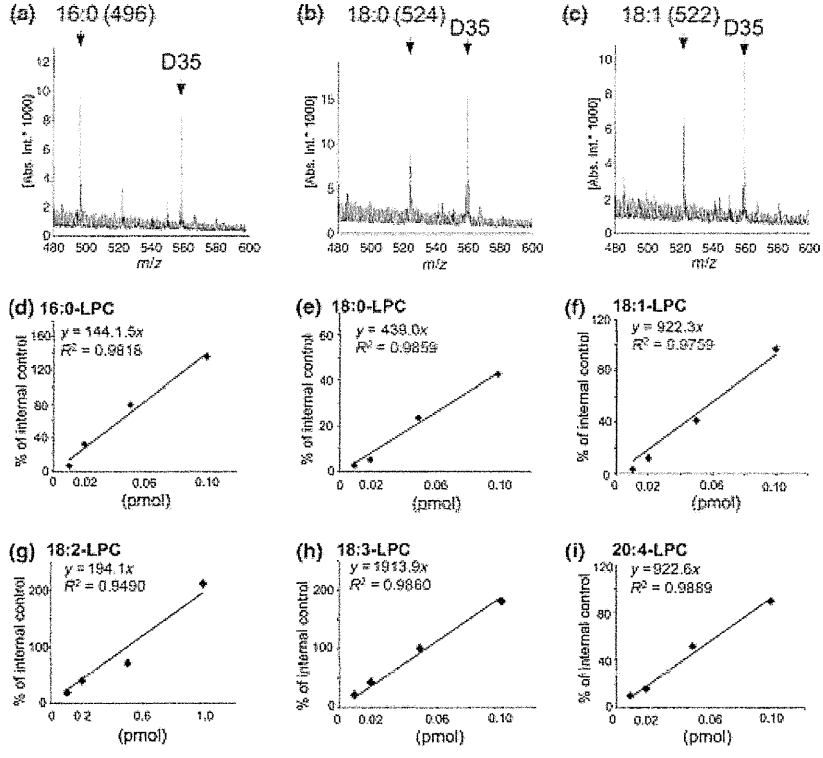

Fig. 1 Standard curve of LPC species by NALDI-TOF-MS. (a–c) Representative charts of mass spectra with authentic standard reagents, 16:0-, 18:0-, 18:1-LPC, and internal standard D35-LPC at the level of 0.1 pmol/well. (d–i) Dose-related signal level of lysophosphatidyl choline (LPC) homologues as compared with corresponding internal standards. Different amounts (0.01–1 pmol) of 16:0-LPC (d), 18:0-LPC (e), 18:1-LPC (f), 18:2-LPC (g), 18:3-LPC (h) and 20:4-LPC (i) were mixed with a fixed amount of D35 LPC (0.1 pmol) in 1 μL of methanol and subjected to NALDI-TOF-MS.

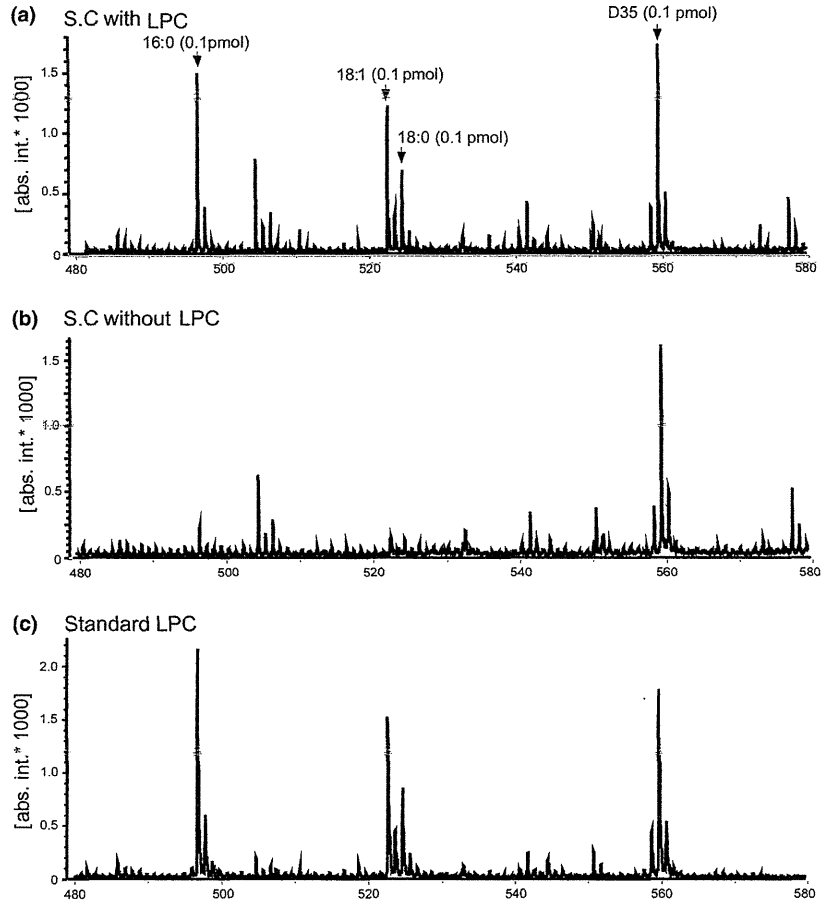

Fig. 2 Recovery yields of authentic LPC species. Representative charts of mass spectra of partially purified samples from the spinal dorsal horn with or without authentic standard: Results represent the mass spectra of partially purified materials from the dorsal half of spinal cord. NALDI-TOF-MS analysis was performed using an Ultraflex I™ TOF/TOF systems in positive ion mode. Numbers above ion peaks indicate their *m/z* values. (a) Authentic LPC mixture (16:0-, 18:0-, and 18:1-LPC) in a dose of 2 nmol each was added to the homogenates of spinal cord. To adjust the concentration to a standard curve levels, 1 μL from 50 μL of finally obtained methanol solution was diluted with 400 μL of methanol. One microliter of the sample applied on NALDI-TOF-MS analysis. (b) Authentic LPC was not added to the homogenates. (c) Standard LPC mixture (0.1 pmol each) was spotted to the NALDI-plate with finally purified materials. The internal standard D35-LPC in a dose of 0.1 pmol was spotted to the plate in all samples.

nerve, followed by homogenization in phosphate-buffered saline and methanol/chloroform extraction. The sample was used for NALDI-TOF-MS analysis. The representative mass spectra of the samples from contralateral (control side) or ipsilateral (injured side) spinal cord are shown (Fig. 3). Marked increases in the ion-signal were observed at m/z 496, 522, 524 and 578 (Fig. 3). Although the signal at *m/z* 504 was decreased (Fig. 3b), this change was not reproduced after repeated trials.

Structure determination of LPC species by MS/MS analysis

MS/MS analyses were performed to determine the structure of molecular ions. When the signal at *m/z* 496 was applied with stronger laser energy at 4.0–6.0 μJ, fragment signals at *m/z* 104, derived from choline, m/z 184, derived from phosphocholine and m/z 313, derived from 16:0 monoacyl glycerol in addition to the original one at *m/z* 496 (Fig. 4a). By use of the database search of the LIPID MAPS and the Lipid Search as previously reported (Hsu and Turk 2003; Pulfer and Murphy 2003; Koizumi *et al.* 2010), the signal at *m/z* 496 was deduced as 16:0-LPC. Similar analysis applied to *m/z* 524 also revealed that there were three fragment signals at *m/z* 104, 184 and 341, and it was deduced as 18:0-LPC (Fig. 4b). Although stronger laser energy treatment of the signal at *m/z* 522 produced fragment signal at 104 and 184, but not the residual signal at *m/z* 339 derived from monoacyl glycerol, it could be also deduced as 18:1 LPC (Fig. 4c).

Time-dependent elevation of nerve injury-induced production of LPC

When the ipsilateral side of spinal cord was isolated at various time points up to 180 min after the nerve injury, there was a significant increase in the level of 16:0-LPC only at 75 min (Fig. 5a). However, there was no significant change on the contralateral side of spinal cord. As autotaxin (ATX), which has lysophospholipase D activity and converts LPC to LPA, plays a key role in nerve injury-induced LPA production (Aoki *et al.* 2008; Ma *et al.* 2010b), we used $atx^{+/-}$-mice to study the effect of ATX on the LPC production. The injury-induced increase in 16:0-LPC was further enhanced in the preparation from the ipsilateral spinal cord from $atx^{+/-}$-mice, but not from the contralateral preparation. The peak effect was observed at 120 min after

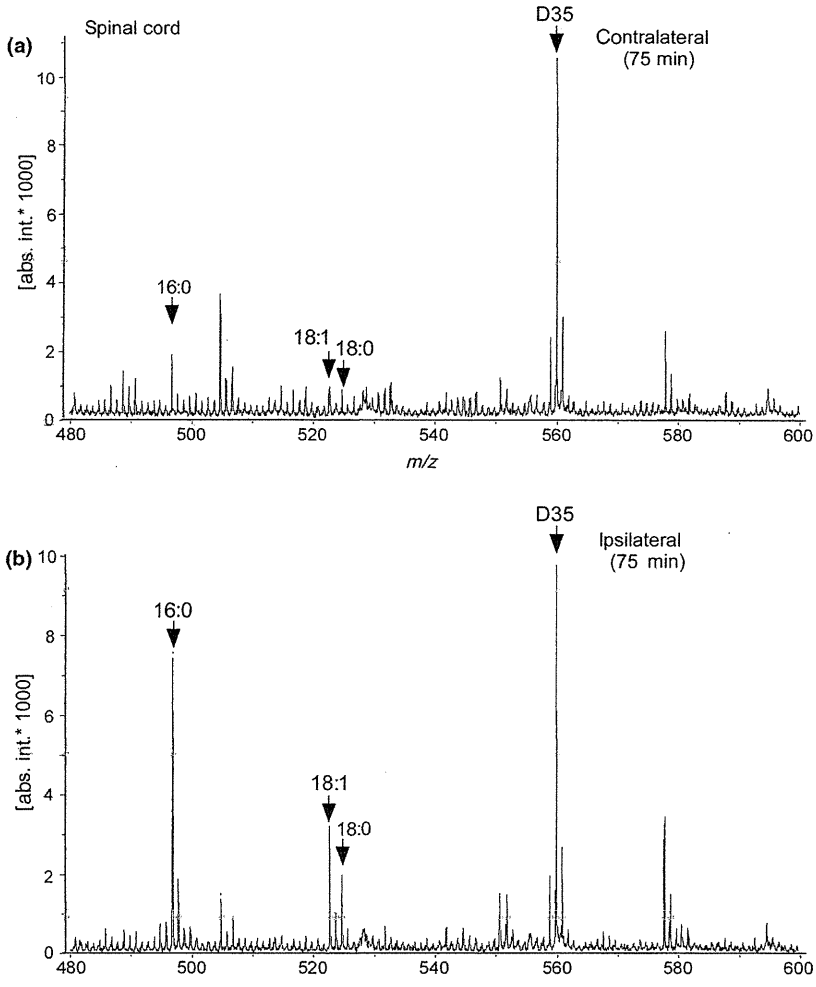

Fig. 3 Biosynthesis of LPC following nerve injury. Representative charts of mass spectra of spinal dorsal horn samples from mice treated with or without SCNI. Results represent the mass spectra of partially purified materials from the contralateral (a) and ipsilateral dorsal half (b) of spinal cord at 75 min after nerve injury.

the injury. The maximum level of 16:0-LPC from $atx^{+/-}$-mice was 240 pmol/mg tissue, which was higher than that from WT-mice (202 pmol/mg tissue). However, the levels at 75 min from $atx^{+/-}$- and WT-mice were equivalent. Quite similar changes were also observed in the cases with 18:0-LPC and 18:1-LPC (Fig. 5b and c).

In the dorsal root, however, injury-induced increase in the preparation from WT mice was also maximal at 75 min in all three species of LPC (Fig. 5d and f). These changes were calculated as 50–100 pmol/mg tissue, which are slightly lower than the case with spinal cord. The peak effect in LPC production at the dorsal root of $atx^{+/-}$-mice was also observed at 120 min, but the increase was less than the case with spinal cord.

When the levels of three species of LPC (16:0-, 18:0- and 18:1-LPC) were combined, the conclusion became clearer. The peak-time increase in LPC following injury in both spinal cord and dorsal root of WT mice was 75 min after the nerve injury. As shown in Fig. 5g and h, the injury increased the LPC level from 308 (at 0 min) to 552 pmol/mg tissue (at 75 min) in the spinal cord (8 mg tissue) of WT mice, while from 288 (at 0 min) to 450 pmol/mg tissue (at 75 min) in the dorsal root (4 mg tissue). Thus, the increase in LPC levels in the spinal cord of WT mice was calculated to be approximately three times higher than that in the dorsal root, and the levels in both spinal cord and dorsal root of $atx^{+/-}$-mice at 120 and 180 min appear to be higher than those in WT mice, although no significant change was observed at 75 min.

Morphine pre-treatment blocks nerve injury-induced LPC production

When morphine at a dose of 3 nmol/5 μL was intracerebroventricularly administered 30 min prior to the nerve injury, nerve injury-induced increase in 16:0-, 18:0- and 18:1-LPC production at 75 min in the spinal cord was all abolished, while there were no significant changes in other ion-peaks (Fig. 6). Quantitative analyses revealed that the morphine pre-treatment completely abolished the injury-induced production of these three LPC species in the dorsal root as well as spinal cord (Fig. 7).

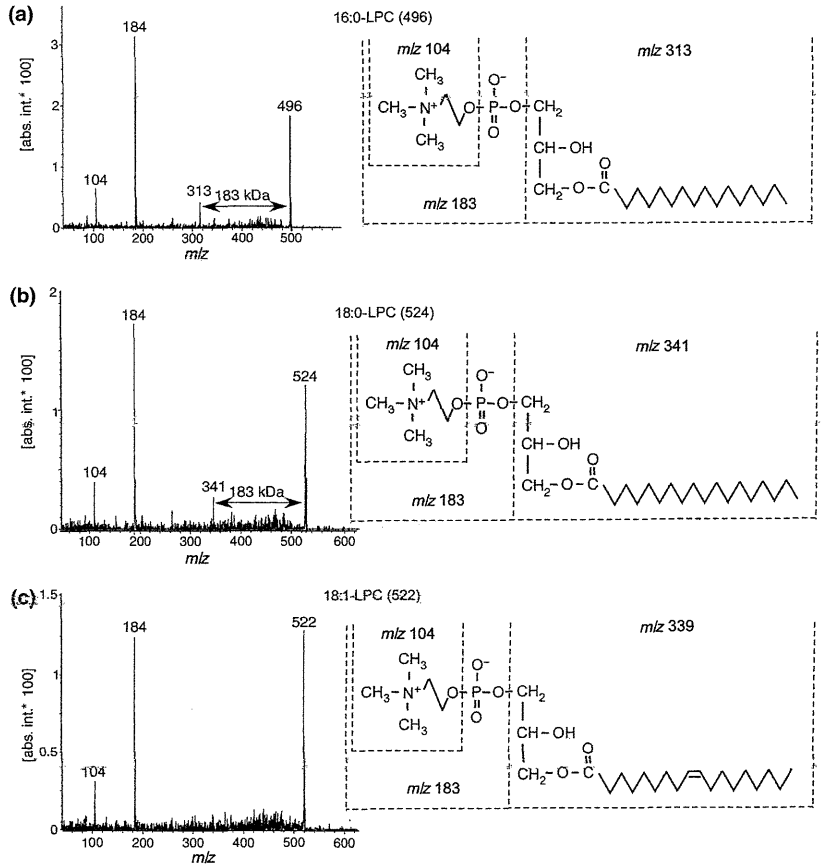

Fig. 4 Structure determination of LPC species by MS/MS analysis MS/MS analyses of ion peaks at *m/z* 496 (a), *m/z* 524 (b), *m/z* 522 (c), obtained from the spinal cord samples with SCNI: Results represent spectra of product ions (left panels) and determined structures deduced by database search (right panel).

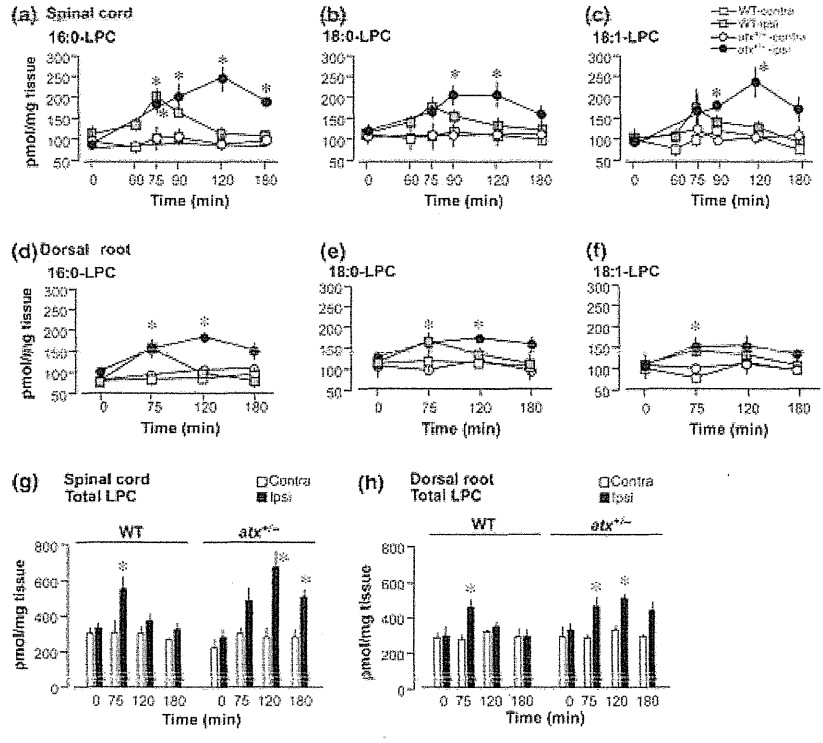

Fig. 5 Time course of LPC levels in spinal cord and dorsal root following nerve injury of WT or *atx*$^{+/-}$ -mice. (a–f) The contents of each species of LPC (16:0-, 18:0-, 18:1-LPC) as pmol/mg tissue weight of spinal cord (a–c) or dorsal root (d–f) preparations at various time-points after the injury of WT and *atx*$^{+/-}$ mice were quantified. (g, h) The combined contents of three LPC species from spinal cord (g) or dorsal root (h) were quantified. Data are expressed as the mean ± SEM from experiments using 3–6 mice. $^{*}p < 0.05$, versus contralateral preparations.

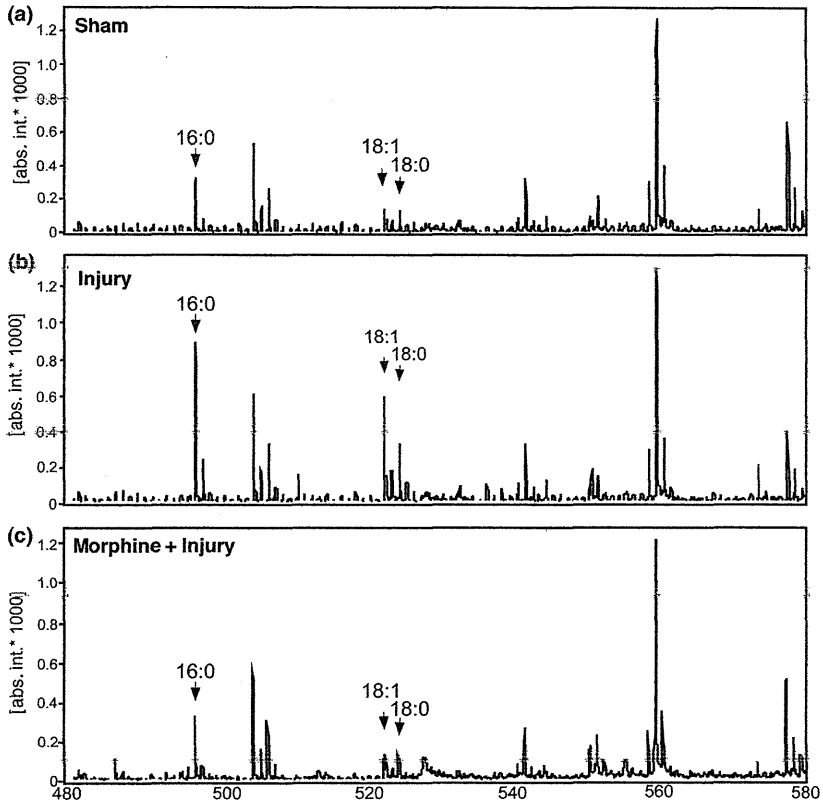

Fig. 6 Pre-emptive inhibition of injury-induced LPC production by morphine. The representative chart of mass spectra of spinal cord preparations treated with sham-operation (a), SCNI (b) and morphine administration (3 nmol, i.c.v.) 30 min prior to SCNI (c) are shown.

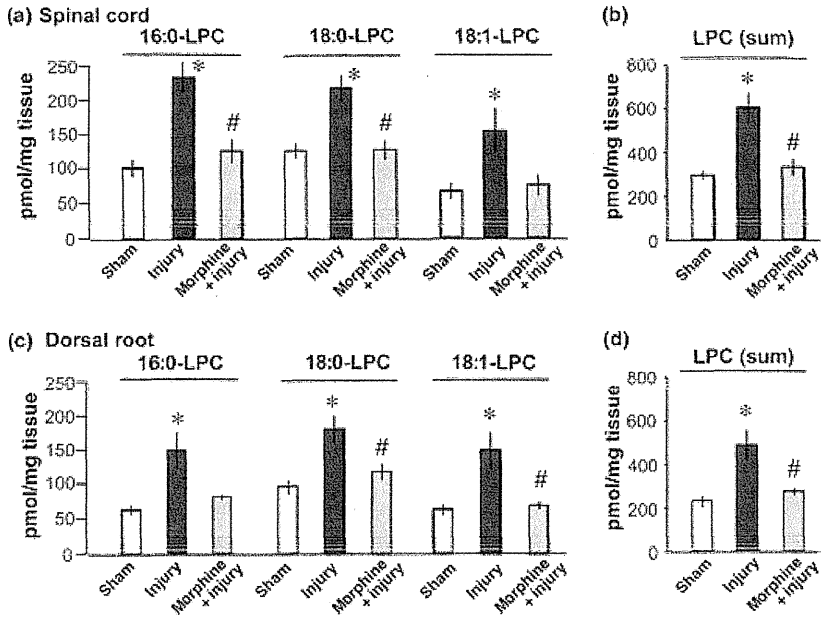

Fig. 7 Quantitative analysis of injury-induced LPC production and its inhibition by morphine pre-treatment. The tissue content of LPC species in spinal cord (a, b) or dorsal root preparations (c, d) treated with injury with or without morphine pre-treatment are quantified. Data are expressed as the mean ± SEM from experiments using 3–6 mice. $^{*}p < 0.05$, versus sham-operation preparations. $^{\#}p < 0.05$, versus injury-operation preparations.

Discussion

The present study shows that the successful simultaneous measurement of several species of LPC molecules by use of NALDI-TOF-MS analysis, which has been developed recently as a matrix-free/surface-assisted alternative to matrix-assisted laser desorption/ionization-TOF-MS (Wyatt *et al.* 2010). This new MS analysis enables to minimize the

background signal ion-peaks in the low molecular region observed in the case with matrix-assisted laser desorption/ionization-TOF-MS (Wyatt *et al.* 2010) and seems to have some advantages in terms of simple and rapid procedures, compared to the case with liquid chromatography–MS, which requires the determination of separation condition for each species of LPC molecules (Morishige *et al.* 2010). In terms of resolution and identification of each species of LPC molecules, there was no substantial problem by use of MS–MS analysis of each signal ion-peak and following data base search. Most important issue was the relatively high yield of recovery from the fresh tissues (spinal cord and dorsal root). By simplifying the extraction and purification processes, we succeeded in the establishment of 70–89% recovery. The species of LPC molecules we obtained from these preparations were saturated LPC molecules such as 16:0-LPC, 18:0-LPC and 18:1-LPC, but not highly unsaturated LPC molecules such as 18:2-LPC, 18:3-LPC or 20:4-LPC or LPC molecules with longer chain, which are detected in plasma (Takatera *et al.* 2006). There is a report that saturated and unsaturated fatty acids are mainly located at the position of sn-1 and sn-2, respectively (Yamashita *et al.* 1997). Thus, it is speculated that phospholipase A_2 (PLA_2) plays important roles in the injury-induced generation of LPCs than PLA_1. This speculation is consistent to previously observation that nerve injury causes an activation of PLA_2 in the spinal cord within 60 min (Ma *et al.* 2010b).

A series of our studies have revealed that LPA and LPA_1 receptor signaling play key roles in the initiation of nerve injury-induced neuropathic pain and its underlying mechanisms such as demyelination of dorsal root, up-regulation of $Ca_V\alpha2\delta1$ in DRG and protein kinase Cγ in the dorsal horn (Inoue *et al.* 2004; Ueda 2006, 2008). Most recently, we have reported that LPA production evaluated by biological assay using B103 cells expressing LPA_1 occurs only in the ipsilateral dorsal horn and dorsal root, but not in the spinal and sciatic nerve or in corresponding contralateral regions (Ma *et al.* 2010b). These findings are consistent with the finding that nerve injury-induced LPA_1-mediated demyelination was only observed in the ipsilateral dorsal root, but not spinal nerve or sciatic nerve (Ma *et al.* 2010b; Nagai *et al.* 2010), suggesting that LPA produced in the spinal cord is transported, but does not diffuse to the dorsal root. In addition, we observed that the LPA production was also reproduced in the *in vitro* study using spinal cord slices by the combined application of substance P and NMDA, which are supposed to mimic intense nociceptive transmission (Inoue *et al.* 2008b). As the presence of ATX was essential for LPA production in these studies, the ATX-mediated conversion of LPC appears to be involved in the LPA production, being consistent to the findings that nerve injury-induced demyelination and neuropathic pain were significantly attenuated in $atx^{+/-}$-mice (Inoue *et al.* 2008a; Ma *et al.* 2009b; Nagai *et al.* 2010). A recent report demonstrated that significant amounts of ATX are present in the cerebrospinal fluid, but the levels of LPC and LPA are very low, suggesting that extracellular LPC production would be a rate-limiting step for LPA production (Nakamura *et al.* 2009). In addition, as the measurement of LPA requires negative mode in MS analysis, which is much less sensitive than the case with positive mode used for LPA measurement (Tanaka *et al.* 2004), we were unable to directly measure LPA in the present study.

For these reasons, we attempted to measure the change in LPC levels after the nerve injury. In the time–course study, it was revealed that the levels of 16:0-LPC, 18:0-LPC and 18:1-LPC in the spinal cord and dorsal horn were all significantly increased at 75 min after the nerve injury, but followed by rapid decline. Most interestingly, these levels were further increased at 120 min in $atx^{+/-}$-mice, although they were substantially equivalent to those in WT-mice at 75 min. The fact that ATX-mediated conversion of LPC to LPA (deduced from the detected losses of LPC) is late may be explained by the view that the step of transport of newly generated LPC to ATX in extracellular space or CSF is time-consuming process. But it is unlikely that the activation of ATX is time-consuming, because ATX in CSF from naive mice already possesses activities to convert LPC to LPA (Inoue *et al.* 2008b). This view is consistent to the previous finding that *in vitro* LPA production using spinal cord slices absolutely requires the addition of exogenous ATX (Inoue *et al.* 2008b). The injury-induced increase of LPC in the ipsilateral dorsal root/mouse was approximately 30% of ipsilateral dorsal half of spinal cord. Thus, it is suggested that LPC in its form is transported to and converted to LPA at the dorsal root, taking into account the previous findings that injury-induced LPA production and LPA_1-mediated demyelination were only observed in the dorsal root, but not spinal nerve or sciatic nerve (Ma *et al.* 2010b; Nagai *et al.* 2010). However, the possibility that injury-induced LPC production occurs in the dorsal root as well as spinal cord cannot be excluded. The fact that peak effects of LPC production in $atx^{+/-}$-mice were observed at 120 min after the injury was consistent with the pharmacological study to see the blockade of nerve injury-induced neuropathic pain using Ki16425, a short-lived LPA_1 antagonist (Ma *et al.* 2009a).

The most important finding is that the pre-treatment with morphine abolished the nerve injury-induced elevation of LPC levels. Nerve injury-induced neuropathic pain has a nature to sustain for at least several weeks. It is accepted that this nature is closely related to memory processes, which include long-term potentiation at the level of dorsal horn and brain, long-lasting genetic and epigenetic changes in DRG neurons (Navarro *et al.* 2007; Zhuo 2007; Uchida *et al.* 2010) and sustained cytokine networks among neurons, astrocytes and microglia (Scholz and Woolf 2007; Milligan and Watkins 2009). Therefore, the complete inhibition of intense nociceptive signal may prevent such memory

processes for the manifestation of neuropathic pain. The pre-emptive morphine analgesia in clinic is based on this concept (Richmond *et al.* 1993). Indeed, we have successfully reproduced similar pre-emptive analgesia in the experimental animal model, in which systemic and central pre-treatments with morphine abolished the nerve injury-induced neuropathic pain (Rashid and Ueda 2005). In this report, the administration of morphine 30 min prior to nerve injury completely abolished neuropathic pain and its underlying mechanisms such as long-lasting PKCγ up-regulation in the dorsal horn. Thus, the present finding showing the central morphine-induced complete blockade of nerve injury-induced elevation of LPC may be related to the concept of pre-emptive analgesia, because LPA converted from LPC plays key roles in the initiation of neuropathic pain (Inoue *et al.* 2004; Ueda 2008). The direct evidence measuring LPA would be the next subject to support this view.

In conclusion, the present study firstly demonstrates the simultaneous MS analysis of several species of LPC molecules, and the nerve injury-induced elevation of LPC, which is likely modified by the *in vivo* conversion to LPA by ATX. In addition, the morphine pre-treatment to block the nociceptive signal abolishes the nerve injury-induced LPC production, underlying the mechanisms for pre-emptive analgesia.

Acknowledgements

We would like to thank Dr Junken Aoki (Tohoku Univ) for generous gift of *atx*$^{+/-}$ mice, Tomoyo Ogawa and Makoto Inoue for technical help. Parts of this work were supported by MEXT KAKENHI (17109015 to Hiroshi Ueda). AstraZeneca Foundation, and Health Labor Sciences Research Grants from the Ministry of Health, Labor and Welfare of Japan (to Hiroshi Ueda): 'Research on Allergic disease and Immunology' and 'Third Term Comprehensive Control Research for Cancer (398–49)' also supported this work.

References

Aoki J., Inoue A. and Okudaira S. (2008) Two pathways for lysophosphatidic acid production. *Biochim. Biophys. Acta* **1781**, 513–518.

Basbaum A. I. and Fields H. L. (1979) The origin of descending pathways in the dorsolateral funiculus of the spinal cord of the cat and rat: further studies on the anatomy of pain modulation. *J. Comp. Neurol.* **187**, 513–531.

Bligh E. G. and Dyer W. J. (1959) A rapid method of total lipid extraction and purification. *Can. J. Biochem. Physiol.* **37**, 911–917.

Choi J. W., Herr D. R., Noguchi K. *et al.* (2010) LPA receptors: subtypes and biological actions. *Annu. Rev. Pharmacol. Toxicol.* **50**, 157–186.

Chun J., Hla T., Lynch K. R., Spiegel S. and Moolenaar W. H. (2010) International Union of Basic and Clinical Pharmacology. LXXVIII. Lysophospholipid receptor nomenclature. *Pharmacol. Rev.* **62**, 579–587.

Fields H. L., Basbaum A. I. and Heinricher M. M. (2006) Central nervous system mechanisms of pain modulation, in *Wall and Melzack's Textbook of Pain* (McMahon S. B. and Koltzenburg M. eds), pp. 125–142. Elsevier Churchill Livingstone, Philadelphia.

Hsu F. F. and Turk J. (2003) Electrospray ionization/tandem quadrupole mass spectrometric studies on phosphatidylcholines: the fragmentation processes. *J. Am. Soc. Mass Spectrom.* **14**, 352–363.

Inoue M., Rashid M. H., Fujita R., Contos J. J., Chun J. and Ueda H. (2004) Initiation of neuropathic pain requires lysophosphatidic acid receptor signaling. *Nat. Med.* **10**, 712–718.

Inoue M., Ma L., Aoki J., Chun J. and Ueda H. (2008a) Autotaxin, a synthetic enzyme of lysophosphatidic acid (LPA), mediates the induction of nerve-injured neuropathic pain. *Mol. Pain* **4**, 6.

Inoue M., Ma L., Aoki J. and Ueda H. (2008b) Simultaneous stimulation of spinal NK1 and NMDA receptors produces LPC which undergoes ATX-mediated conversion to LPA, an initiator of neuropathic pain. *J. Neurochem.* **107**, 1556–1565.

Koizumi S., Yamamoto S., Hayasaka T., Konishi Y., Yamaguchi-Okada M., Goto-Inoue N., Sugiura Y., Setou M. and Namba H. (2010) Imaging mass spectrometry revealed the production of lyso-phosphatidylcholine in the injured ischemic rat brain. *Neuroscience* **168**, 219–225.

Lin M. E., Herr D. R. and Chun J. (2010) Lysophosphatidic acid (LPA) receptors: signaling properties and disease relevance. *Prostaglandins Other Lipid Mediat.* **91**, 130–138.

Ma L., Matsumoto M., Xie W., Inoue M. and Ueda H. (2009a) Evidence for lysophosphatidic acid 1 receptor signaling in the early phase of neuropathic pain mechanisms in experiments using Ki-16425, a lysophosphatidic acid 1 receptor antagonist. *J. Neurochem.* **109**, 603–610.

Ma L., Uchida H., Nagai J., Inoue M., Chun J., Aoki J. and Ueda H. (2009b) Lysophosphatidic acid-3 receptor-mediated feed-forward production of lysophosphatidic acid: an initiator of nerve injury-induced neuropathic pain. *Mol. Pain* **5**, 64.

Ma L., Nagai J. and Ueda H. (2010a) Microglial activation mediates de novo lysophosphatidic acid production in a model of neuropathic pain. *J. Neurochem.* **115**, 643–653.

Ma L., Uchida H., Nagai J., Inoue M., Aoki J. and Ueda H. (2010b) Evidence for de novo synthesis of lysophosphatidic acid in the spinal cord through phospholipase A2 and autotaxin in nerve injury-induced neuropathic pain. *J. Pharmacol. Exp. Ther.* **333**, 540–546.

Malmberg A. B. and Basbaum A. I. (1998) Partial sciatic nerve injury in the mouse as a model of neuropathic pain: behavioral and neuroanatomical correlates. *Pain* **76**, 215–222.

Milligan E. D. and Watkins L. R. (2009) Pathological and protective roles of glia in chronic pain. *Nat. Rev. Neurosci.* **10**, 23–36.

Morishige J., Urikura M., Takagi H., Hirano K., Koike T., Tanaka T. and Satouchi K. (2010) A clean-up technology for the simultaneous determination of lysophosphatidic acid and sphingosine-1-phosphate by matrix-assisted laser desorption/ionization time-of-flight mass spectrometry using a phosphate-capture molecule, Phos-tag. *Rapid Commun. Mass Spectrom.* **24**, 1075–1084.

Nagai J., Uchida H., Matsushita Y., Yano R., Ueda M., Niwa M., Aoki J., Chun J. and Ueda H. (2010) Autotaxin and lysophosphatidic acid1 receptor-mediated demyelination of dorsal root fibers by sciatic nerve injury and intrathecal lysophosphatidylcholine. *Mol. Pain* **6**, 78.

Nakamura K., Ohkawa R., Okubo S. *et al.* (2009) Autotaxin enzyme immunoassay in human cerebrospinal fluid samples. *Clin. Chim. Acta* **405**, 160–162.

Navarro X., Vivo M. and Valero-Cabre A. (2007) Neural plasticity after peripheral nerve injury and regeneration. *Prog. Neurobiol.* **82**, 163–201.

Noguchi K., Herr D., Mutoh T. and Chun J. (2009) Lysophosphatidic acid (LPA) and its receptors. *Curr. Opin. Pharmacol.* **9**, 15–23.

Pulfer M. and Murphy R. C. (2003) Electrospray mass spectrometry of phospholipids. *Mass Spectrom. Rev.* **22**, 332–364.

Rashid M. H. and Ueda H. (2005) Pre-injury administration of morphine prevents development of neuropathic hyperalgesia through activation of descending monoaminergic mechanisms in the spinal cord in mice. *Mol. Pain* **1**, 19.

Richmond C. E., Bromley L. M. and Woolf C. J. (1993) Preoperative morphine pre-empts postoperative pain. *Lancet* **342**, 73–75.

Sato M. and Takagi H. (1971) Enhancement by morphine of the central descending inhibitory influence on spinal sensory transmission. *Eur. J. Pharmacol.* **14**, 60–65.

Scholz J. and Woolf C. J. (2007) The neuropathic pain triad: neurons, immune cells and glia. *Nat. Neurosci.* **10**, 1361–1368.

Sutphen R., Xu Y., Wilbanks G. D. *et al.* (2004) Lysophospholipids are potential biomarkers of ovarian cancer. *Cancer Epidemiol. Biomarkers Prev.* **13**, 1185–1191.

Takatera A., Takeuchi A., Saiki K., Morisawa T., Yokoyama N. and Matsuo M. (2006) Quantification of lysophosphatidylcholines and phosphatidylcholines using liquid chromatography-tandem mass spectrometry in neonatal serum. *J. Chromatogr. B Analyt. Technol. Biomed. Life Sci.* **838**, 31–36.

Tanaka T., Tsutsui H., Hirano K., Koike T., Tokumura A. and Satouchi K. (2004) Quantitative analysis of lysophosphatidic acid by time-of-flight mass spectrometry using a phosphate-capture molecule. *J. Lipid Res.* **45**, 2145–2150.

Tanaka M., Okudaira S., Kishi Y. *et al.* (2006) Autotaxin stabilizes blood vessels and is required for embryonic vasculature by producing lysophosphatidic acid. *J. Biol. Chem.* **281**, 25822–25830.

Tokumura A. (2002) Physiological and pathophysiological roles of lysophosphatidic acids produced by secretory lysophospholipase D in body fluids. *Biochim. Biophys. Acta* **1582**, 18–25.

Uchida H., Ma L. and Ueda H. (2010) Epigenetic gene silencing underlies C-fiber dysfunctions in neuropathic pain. *J. Neurosci.* **30**, 4806–4814.

Ueda H. (2006) Molecular mechanisms of neuropathic pain-phenotypic switch and initiation mechanisms. *Pharmacol. Ther.* **109**, 57–77.

Ueda H. (2008) Peripheral mechanisms of neuropathic pain – involvement of lysophosphatidic acid receptor-mediated demyelination. *Mol. Pain* **4**, 11.

Ueda H. (2011) Lysophosphatidic acid as initiator of neuropathic pain - biosynthesis and demyelination. *Clin. Lipidol.* **6**, 147–158.

Wyatt M. F., Ding S., Stein B. K., Brenton A. G. and Daniels R. H. (2010) Analysis of various organic and organometallic compounds using nanostructure-assisted laser desorption/ionization time-of-flight mass spectrometry (NALDI-TOFMS). *J. Am. Soc. Mass Spectrom.* **21**, 1256–1259.

Yamashita A., Sugiura T. and Waku K. (1997) Acyltransferases and transacylases involved in fatty acid remodeling of phospholipids and metabolism of bioactive lipids in mammalian cells. *J. Biochem.* **122**, 1–16.

Zhuo M. (2007) A synaptic model for pain: long-term potentiation in the anterior cingulate cortex. *Mol. Cells* **23**, 259–271.

Zimmermann M. (1983) Ethical guidelines for investigations of experimental pain in conscious animals. *Pain* **16**, 109–110.

Current Topics

Lipid Mediators and Pain Signaling

Lysophosphatidic Acid as the Initiator of Neuropathic Pain

Hiroshi UEDA

Division of Molecular Pharmacology and Neuroscience, Nagasaki University Graduate School of Biomedical Sciences; 1–14 Bunkyo-machi, Nagasaki 852–8521, Japan.

Received February 15, 2011

The injury-induced intense stimulation of spinal cord neurons causes lysophosphatidic acid (LPA) biosynthesis. LPA_1 receptor activation causes demyelination and sprouting of dorsal root fibers, leading to an induction of synaptic reorganization underlying allodynia, in which innocuous (tactile) stimuli cause intense pain. The LPA_1 signal also initiates the up-regulation of $Ca_v\alpha2\delta1$ in dorsal root ganglion and PKCγ in the dorsal horn, underlying mechanisms for characteristic neuropathic hyperalgesia in myelinated sensory (A-type) fibers. On the other hand, the LPA_3 receptor mediates microglia activation at the early stage after nerve injury and LPA-induced LPA biosynthesis. Thus, both the LPA_1 and LPA_3 receptors play key roles in the initiation step using a feed-forward system for neuropathic pain.

Key words lysophosphatidic acid; demyelination; feed-forward system; neuropathic pain; microglia

1. INTRODUCTION

Chronic pain should be considered disease pain, though acute or nociceptive pain is sometimes viewed as physiological pain because of its bio-alarming roles. Neuropathic pain is a representative chronic pain, and is caused by damage to peripheral or central neurons in the pain pathway.[1—4] This type of chronic pain commonly occurs as a secondary symptom in diseases such as diabetes, cancer, and herpes zoster infection, or as a side effect of chemotherapeutic treatments.[5—8] Neuropathic pain following partial sciatic nerve injury is often characterized by abnormally hypersensitive sensory perception through A-fibers, called hyperalgesia or allodynia, in which innocuous (tactile) stimuli cause intense pain.[9,10] The abnormal sensory perception also includes C-fiber hypoesthesia,[10—12] which indicates sensory loss.[13,14] A number of studies[10,12,15] demonstrate the altered expression of receptors, neuropeptides and ion-channels in sensory fiber neurons, called dorsal root ganglion (DRG) and in the dorsal horn. According to current studies, on the other hand, the sustained activation of non-neuronal cells such as astrocytes and microglia becomes manifest in the mechanisms underlying neuropathic pain.[9,11] In addition to these mechanisms, the demyelination is supposedly related to chronic pain diseases, and to the physical cross-talk/sprouting and ectopic discharge in sensory fibers, all which may underlie neuropathic hyperalgesia and allodynia.[10,12,16] As neuropathic pain is in general resistant to non-steroidal anti-inflammatory drugs (NSAIDs) or morphine, it has been called intractable pain, though a limited number of medicines are currently available or in progress of development in clinics.[17]

Accumulating findings reveal the important insights into both the basic biology and biomedical importance of signaling initiated by lipid mediator lysophosphatidic acid (1-acyl 2-hydroxyl glycerol 3-phosphate, LPA), LPA, a simple lipid with glycerol, fatty acid and phosphate in its structure. LPA plays roles in many cellular processes including cellular proliferation, cell migration, prevention of apoptosis, cytokine and chemokine secretion and smooth muscle contraction.[18—21] LPA receptors activate multiple signaling pathways and multiple G-proteins,[22,23] but LPA_1 signaling is unique, since it has a downstream coupling to $G\alpha_{12/13}$, as well as $G_{i/o}$ and $G_{q/11}$. Regarding neurobiological actions, LPA causes a growth cone collapse on neurons through its receptor LPA_1 and downstream $G\alpha_{12/13}$-RhoA-Rho kinase (ROCK) system,[24,25] and plays crucial roles in neuronal developmental processes, including neurogenesis, neuronal migration, neuritogenesis and myelination.[26,27] In terms of pain regulation, we first reported that LPA causes an activation of peripheral nociceptor endings directly and indirectly through a release of histamine from peripheral cells, such as mast cells.[28,29] Current studies have revealed that LPA plays a key role in the initiation of neuropathic pain.[10,12,30] As the intrathecal LPA-induced abnormal pain shows quite similar characteristics to those in nerve injury-induced neuropathic pain,[30] LPA could be considered as a good tool for the studies of *in vitro* and *in vivo* mechanisms underlying neuropathic pain.[31—37]

2. LPA_1-MEDIATED INITIATION OF NEUROPATHIC PAIN

Among multiple mechanisms involved in the manifestation of nerve injury-induced neuropathic pain, the enhanced expression of $Ca_v\alpha2\delta1$ expression in DRG, PKCγ expression and microglial activation in dorsal horn seem to be representative mechanisms for hyperalgesia, while the demyelination and following physical cross-talk among sensory fibers may underlie the mechanisms for allodynia. We were the first to find that nerve injury-induced neuropathic pain behaviors were substantially abolished in $lpa_1^{-/-}$ mice.[30] As there was no significant change in the basal nociceptive threshold, it is evident that endogenous levels of LPA do not affect this threshold and that newly produced LPA following nerve injury causes neuropathic pain mechanisms. In order to study the critical time period for LPA_1 receptor-mediated sig-

e-mail: ueda@nagasaki-u.ac.jp

naling underlying neuropathic pain and its mechanisms, Ki-16425, a short-lived antagonist of LPA_1 receptor was used.[33] The Ki-16425 blockade of nerve injury-induced neuropathic pain and upregulation of $Ca_v\alpha2\delta1$ expression was maximal as late as 3 h after the injury but not after this critical period. These results suggest that LPA_1 signaling, which underlies the development of neuropathic pain, works at an early stage of the critical period after nerve injury.

3. LPA_1-MEDIATED UPREGULATION OF KEY MOLECULES UNDERLYING HYPERALGESIA

Upregulation of $Ca_v\alpha2\delta1$ expression and subsequent increased pain transmission may underlie the mechanism for hyperalgesia. Gabapentin and pregabalin, which are widely used in clinics for neuropathic pain, are known to inhibit the pain transmission by inhibiting this subunit $Ca_v\alpha2\delta$ activity.[38] The expression of $Ca_v\alpha2\delta1$ is observed only in the small C-fiber neurons of DRG in naïve animals.[8] After partial injury of the sciatic nerve, most of the A-fiber neurons also express this subunit.[30] Pretreatment with Clostridium botulinum C3 exoenzyme (BoNT/C3), an inhibitor of RhoA, abolished this additional expression in A-fiber neurons. Quite similar results of additional $Ca_v\alpha2\delta1$ expression in these neurons and its blockade by BoNT/C3 were observed when LPA was intrathecally injected only once. On the other hand, the nerve injury- or LPA-induced up-regulation of $Ca_v\alpha2\delta1$ was abolished in $lpa_1^{-/-}$ mice.[10,30]

N-Methyl-D-aspartate (NMDA) receptor plays key roles in the transmission of pain in naïve and chronic pain status.[39] Recent studies reported that NMDA receptor is transactivated through EphB signaling initiated by interaction with presynaptic Ephrin B1.[40—42] When the profiling of LPA-induced and BoNT/C3 reversible genes in DRG was performed, *ephrin B1* was found in 82 unique genes.[36] Further characterization revealed that antisense oligonucleotide for *ephrin B1* largely abolished the LPA-induced mechanical allodynia, thermal hyperalgesia and hypersensitivity to electrical stimuli through $A\delta$ and $A\beta$-fibers. As EphrinB1-Fc caused neuropathic pain-like behaviors in an NMDA receptor antagonist MK-801-reversible manner, LPA-mediated Ephrin B1 upregulation may also contribute to the mechanisms underlying neuropathic hyperalgesia.

As seen in the case with nerve injury, intrathecal injection of LPA causes an up-regulation of PKCγ at the substantia gelatinosa of spinal dorsal horn.[30] This change is known as so-called wind-up facilitation or hyperalgesia observed in neuropathic pain.[43] The up-regulation by nerve injury or LPA was also abolished by BoNT/C3 pretreatment and in $lpa_1^{-/-}$ mice.

4. LPA_1-MEDIATED DEMYELINATION UNDERLYING ALLODYNIA

It is known that many demyelinating diseases accompany chronic pain, as seen in the cases with Guillain–Barre syndrome[44] and multiple sclerosis.[45] Demyelination and subsequent physical cross-talk[12,31] and ectopic discharges due to accumulation of sodium channels[46] have been speculated as the mechanisms underlying neuropathic pain. Nerve injury- and intrathecal LPA-induced demyelination of dorsal root fibers through LPA1 receptor activation are evidenced by the down-regulation of myelin proteins, such as myelin basic protein (MBP), myelin protein zero (P0) and myelin-associated glycoprotein (MAG).[31,35,37] The *ex vivo* studies using dorsal root fibers also demonstrated that the addition of LPA causes demyelination within 24 h in scanning and transmission electron microscopy (SEM and TEM) analyses.[31] As well as typical demyelination of A-fibers, there was direct contact between neighboring C-fibers.[31] In co-culture experiments using myelinated fibers built up with isolated DRG neurons and Schwann cells, the addition of LPA also causes a sequential morphological change, in an order of collapse of growth cone at 1 h, sprouting at the nerve endings at 8 h and axon at 18 h and complete spreading of myelinated Schwann cell at 36 h.[47] As the down-regulation of myelin proteins was abolished by the pretreatment with BoNT/C3 or ROCK inhibitor Y-27632, the major pathway is presumably mediated by the LPA_1-$G_{12/13}$-RhoA-ROCK system. Indeed, the LPA-induced down-regulation of myelin protein genes in *in vivo* and *ex vivo* studies using dorsal root fibers was abolished by Y-27632.[30] Most recently, there is a report that c-Jun plays a negative regulator role in the myelin protein gene expression.[48,49] As the RhoA-ROCK system is reported to stimulate c-*jun* expression through JNK activation,[50] it is speculated that the sequential activation of LPA_1-$G_{12/13}$-RhoA-ROCK-JNK, followed by up-regulation of c-*jun*, leads to a negative regulation of myelin protein gene expression. In terms of signal transduction, it is also known that LPA_1 causes the stress-fiber formation and actin rearrangement through $G_{12/13}$-RhoA-ROCK activation.[51,52] Thus, such LPA_1-mediated morphological changes may contribute to rapid mechanisms underlying demyelination without any changes in myelin protein levels.

However, current studies demonstrated a different mechanism independent of the $G_{12/13}$-RhoA-ROCK system.[37] Intrathecal injection of LPA causes a rapid down-regulation of myelin-associated glycoprotein (MAG). By surveying protease inhibitors, the calcium-activated neutral serine protease, calpain was found to play a major role in the down-regulation of MAG. Pretreatment with calpain inhibitors abolished the MAG down-regulation and significantly attenuated the LPA-induced neuropathic pain-like behaviors. Interestingly, calpain activation in dorsal root was only observed by nerve injury and abolished in $lpa_1^{-/-}$ mice, while it was not observed by the pretreatment with inflammatogenic Complete Freund Adjuvant (CFA). Furthermore, calpain inhibitors reversed the nerve injury-induced neuropathic pain, but not CFA-induced pain. Although details remain elusive, it is suggested that the LPA_1-$G_{q/11}$-PLC activation system may play a role in the calcium-mediated protein degradation. Thus, several cellular mechanisms following LPA_1 stimulation may contribute to the demyelination.

In relation to allodynia, the loss of insulation of sensory fibers following LPA1-mediated demyelination may cause a physical cross-talk (or electric synapse/ephapse) among innocuous $A\beta$ fibers and noxious C- or $A\delta$-fibers,[10,12] which in turn leads to an abnormal pain transmission allodynia. The down regulation of MAG may also cause the sprouting, which is induced by a loss of negative signal through the NOGO/p75 receptor complex,[12] as seen in Fig. 1.

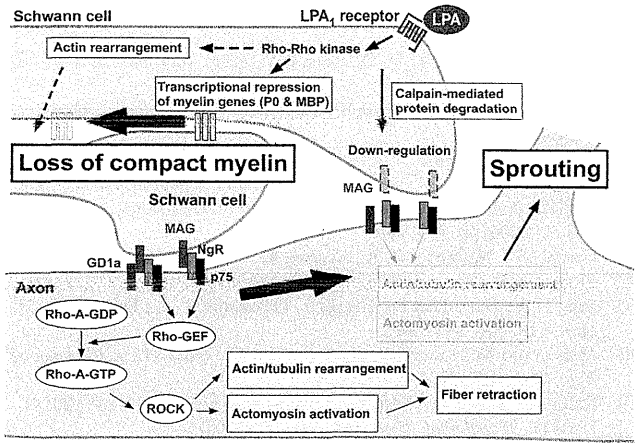

Fig. 1. Schematic Model of LPA_1-Mediated Demyelination and Sprouting

The stimulation of LPA_1 receptor on myelinated Schwann cells causes rapid down-regulation of myelin proteins through calpain-mediated down regulation and gene silencing. The downregulation of compact myelin proteins including myelin binding protein (MBP) and myelin protein zero (P0) leads to a loosening of the myelin sheath. The loss of another myelin protein, myelin associated glycoprotein (MAG), which couples to NOGO/p75 complex (NgR/p75) and RhoA-ROCK system, results in disinhibition of sprouting, possibly through rearrangements of actin and tubulin polymers.

5. LPA_1-MEDIATED SYNAPTIC REORGANIZATION IN PAIN PATHWAY

Extracellular signal-regulated $kinase_{1/2}$ ($ERK_{1/2}$), representing one of the major subfamilies of mitogen-activated protein kinases (MAPKs), is phosphorylated following membrane depolarization and Ca^{2+} influx.[53] It is known that $ERK_{1/2}$ is immediately activated after noxious stimulation in DRG neurons and spinal dorsal horn in a stimulus intensity-dependent manner.[54,55] Therefore, ERK phosphorylation (pERK) could be a biochemical marker of activated neurons, allowing us to visualize the pain-signaling pathways and more objective evidence of neurotransmission. A significant number of neurons at the superficial layer of spinal dorsal horn became pERK-positive following the stimulation of nociceptive C- and Aδ-fibers by use of Neurometer®, while no neuron became pERK-positive by innocuous Aβ stimulation.[56] However, following sciatic nerve injury, Aβ-stimulation showed a significant number of pERK-positive neurons at the superficial layer of dorsal horn, where the innervation with noxious C- or Aδ-fibers is observed. This mechanism seems to explain why the tactile stimuli (through Aβ) cause intense pain. Such nerve injury-induced synaptic reorganization was also abolished in $lpa_1^{-/-}$ mice.[57]

6. LPA_3-MEDIATED LPA BIOSYNTHESIS

The LPA_1-mediated demyelination following partial injury of sciatic nerve was only observed in dorsal root, but not spinal nerve or sciatic nerve.[35] Such dorsal root-specificity was also observed in the down-regulation of myelin-associated glycoprotein (MAG), which plays a key role in the regulation of axonal sprouting.[12] As the addition of LPA causes the demyelination or down-regulation of MAG in all these sensory nerve regions, the dorsal root specificity following sciatic nerve injury seems attributable to the localized LPA production. The most probable source of LPA would be from spinal cord, since the dorsal root as well as spinal cord is within the subarachnoid.

Recent studies demonstrated that the intense stimulation of spinal cord neurons causes synthesis of lysophosphatidyl choline (LPC), which is in turn converted to LPA by lysophospholipase D or autotaxin (ATX).[21,58] In these experiments, the combination of SP and NMDA, both of which cause an activation of representative target receptors for different types of primary afferent neurons, produces LPC.[58] As no significant synthesis of LPC occurs by single application of either compound, it is presumed to require an intense signal caused by nerve injury, but not by regular pain transmission. Recent studies revealed that phosphatidyl choline is converted to LPC by $cPLA_2$ or $iPLA_2$, both of which are regulated by Ca^{2+}-related mechanisms following NK_1 and NMDA receptor activation. Thus produced LPC in the spinal cord is converted to LPA at the spinal cord and dorsal root by an action of ATX leading to demyelination and $Ca_v\alpha 2\delta 1$ up-regulation.[30]

Current studies demonstrated that the intrathecal injection of LPC caused neuropathic pain-like behaviors, and these behaviors were abolished in $lpa_1^{-/-}$ mice or diminished by 50% in $ATX^{+/-}$ mice.[34] The study to examine the biochemical evidence for this LPC-induced LPA production revealed that the amounts of LPA were much higher than that expected from the simple conversion through ATX.[33] Detailed *ex vivo* culture studies using spinal cord slices revealed that LPA-induced amplified production of LPA was abolished in the preparation derived from $lpa_3^{-/-}$ mice. This observation was supported by the behavioral studies, in which nerve injury-induced neuropathic pain was abolished in $lpa_3^{-/-}$ as well as $lpa_1^{-/-}$ mice. Thus, it is suggested that LPA_1 receptor plays direct roles in molecular machineries underlying neuropathic pain, while LPA_3 receptor and ATX play roles in the synthesis of LPA.

7. MICROGLIA-MEDIATED AMPLIFICATION OF LPA BIOSYNTHESIS

It is now considered that microglia and astrocytes as well as neurons have functional roles in the creation and maintenance of chronic neuropathic pain. Spinal cord glial activation seems to be a common underlying mechanism that leads to chronic pain.[59,60] However, it remains to be learned what signal initiates the glial activation, which is assumed to play a key role in the maintenance of neuropathic pain. An attempt to see the effects of LPA in activating microglia revealed that LPA caused an increase in the expression of brain-derived neurotrophic factor (BDNF) in a primary culture of rat microglia, which express LPA_3, but not LPA_1 or LPA_2 receptors.[61] These actions were mediated by a release of ATP through activation of LPA_3, $G_{q/11}$ and phospholipase C. The released ATP or ectopically converted ADP may in turn cause membrane ruffling (a sign of chemotaxis) *via* $P2Y_{12}$ receptors and $G_{i/o}$ activation, and BDNF expression *via* activation of $P2X_4$ receptors. Current studies using the microglia inhibitor minocycline revealed that LPA-induced microglia activation functions in the early stage development, but not in the late stage maintenance of neuropathic pain.[62] In this study, the early treatment with minocycline abolished

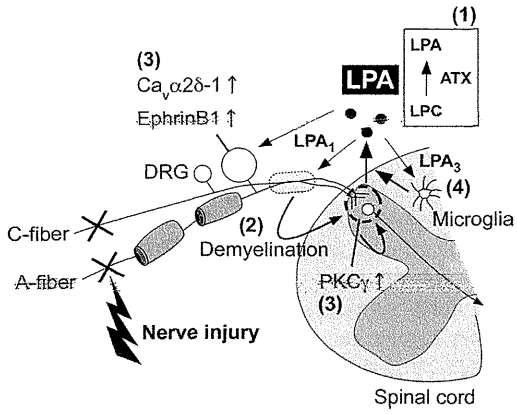

Fig. 2. Working Hypothesis of LPA-Mediated Feed-Forward System Underlying Molecular Mechanisms for Neuropathic Pain

Following (sciatic) nerve injury, intense pain signals activate neurons in spinal dorsal horn and cause a biosynthesis of LPC, which is then converted to LPA by ATX, depicted by (1). Thus produced LPA is transported within 3 h after injury to the ipsilateral side of dorsal root, where it causes demyelination and sprouting, underlying allodynia (2). LPA also causes up-regulation of $Ca_v\alpha2\delta1$ and EphrinB1 in DRG (3), and PKCγ in the spinal dorsal horn, underlying hyperalgesia (3). These mechanisms are believed to cause an activation of spinal neurons, leading to further LPA synthesis, as a feed-forward system. The amplification of LPA biosynthesis also occurs through an activation of LPA_3 receptor and microglia (4). All these mechanisms contribute to the initiation of neuropathic pain.

the LPA-induced and nerve injury-induced neuropathic pain, LPA synthesis and its underlying activation of synthetic enzymes, cytosolic phospholipase A_2 ($cPLA_2$) and calcium-independent PLA_2 ($iPLA_2$). As the post-treatment with minocycline failed to attenuate the established neuropathic pain, microglial activation following LPA_3 signaling seems to take part in the initiation mechanisms for neuropathic pain.

8. CONCLUSION

In the proposed working hypothesis, the LPA-mediated feed-forward system underlying molecular mechanisms for neuropathic pain, the LPA production following intense and mixed pain signals to spinal dorsal horn neurons is the initial mechanism (Fig. 2). Thus produced LPA has two mechanisms: one is related to the actions as an amplifying signal for further LPA production through LPA_3 and microglia activation. The other mechanism is related to the LPA_1-mediated actions as a reverse signal to cause dorsal root demyelination, and upregulation of $Ca_v\alpha2\delta_1$ and Ephrin B_1 in DRG. Demyelination and subsequent sprouting may lead to a pathological pain synapse by Aβ-fibers, underlying allodynia. Up-regulation of key molecules in DRG enhances the pain transmission and may cause subsequent upregulation of PKCγ in the dorsal horn. Enhanced and pathological pain transmission may also contribute to a biosynthesis of LPA through direct and indirect mechanisms. When we consider the drug development to cure neuropathic pain, LPA receptor antagonists or inhibitors of LPA synthesis would be candidates. For this purpose, we need to examine whether this feed-forward system through LPA biosynthesis also occurs in the late phase of neuropathic pain. Assuming that the feed-forward system through LPA synthesis by intense an pain signal (or injury) is true in the central nervous system, the hypothesis may be further extended to central pain induced by various kinds of stress, spinal (brain) injury or stroke.

REFERENCES

1) Apkarian A. V., Baliki M. N., Geha P. Y., *Prog. Neurobiol.*, **87**, 81—97 (2009).
2) Costigan M., Scholz J., Woolf C. J., *Annu. Rev. Neurosci.*, **32**, 1—32 (2009).
3) Saadé N. E., Jabbur S. J., *Prog. Neurobiol.*, **86**, 22—47 (2008).
4) Woolf C. J., Salter M. W., "Textbook of Pain," Chap. 5, 5th ed., ed. by McMahon S., Koltzenburg M., Churchill-Livingstone, New York, U.S.A., 2006, pp. 91—105.
5) Campbell J. N., Meyer R. A., *Neuron*, **52**, 77—92 (2006).
6) Fischer T. Z., Waxman S. G., *Nat. Rev. Neurol.*, **6**, 462—466 (2010).
7) Jung B. F., Herrmann D., Griggs J., Oaklander A. L., Dworkin R. H., *Pain*, **118**, 10—14 (2005).
8) Matsumoto M., Inoue M., Hald A., Xie W., Ueda H., *J. Pharmacol. Exp. Ther.*, **318**, 735—740 (2006).
9) Baron R., Binder A., Wasner G., *Lancet Neurol.*, **9**, 807—819 (2010).
10) Ueda H., *Pharmacol. Ther.*, **109**, 57—77 (2006).
11) Dray A., *Br. J. Anaesth.*, **101**, 48—58 (2008).
12) Ueda H., *Mol. Pain*, **4**, 1—13 (2008).
13) Devigili G., Tugnoli V., Penza P., Camozzi F., Lombardi R., Melli G., Broglio L., Granieri E., Lauria G., *Brain*, **131**, 1912—1925 (2008).
14) Leffler A. S., Hansson P., *Eur. J. Pain*, **12**, 397—402 (2008).
15) Navarro X., Vivó M., Valero-Cabré A., *Prog. Neurobiol.*, **82**, 163—201 (2007).
16) O'Connor A. B., Schwid S. R., Herrmann D. N., Markman J. D., Dworkin R. H., *Pain*, **137**, 96—111 (2008).
17) Dworkin R. H., O'Connor A. B., Audette J., Baron R., Gourlay G. K., Haanpää M. L., Kent J. L., Krane E. J., Lebel A. A., Levy R. M., Mackey S. C., Mayer J., Miaskowski C., Raja S. N., Rice A. S., Schmader K. E., Stacey B., Stanos S., Treede R. D., Turk D. C., Walco G. A., Wells C. D., *Mayo Clin. Proc.*, **85** (Suppl.), S3—S14 (2010).
18) Mills G. B., Moolenaar W. H., *Nat. Rev. Cancer*, **3**, 582—591 (2003).
19) Noguchi K., Herr D., Mutoh T., Chun J., *Curr. Opin. Pharmacol.*, **9**, 15—23 (2009).
20) Park K. A., Vasko M. R., *Trends Pharmacol. Sci.*, **26**, 571—577 (2005).
21) van Meeteren L. A., Moolenaar W. H., *Prog. Lipid Res.*, **46**, 145—160 (2007).
22) Ishii I., Fukushima N., Ye X., Chun J., *Annu. Rev. Biochem.*, **73**, 321—354 (2004).
23) Kingsbury M. A., Rehen S. K., Contos J. J., Higgins C. M., Chun J., *Nat. Neurosci.*, **6**, 1292—1299 (2003).
24) Jalink K., Eichholtz T., Postma F. R., van Corven E. J., Moolenaar W. H., *Cell Growth Differ.*, **4**, 247—255 (1993).
25) Rivera R., Chun J., *Rev. Physiol. Biochem. Pharmacol.*, **160**, 25—46 (2008).
26) Fukushima N., *J. Cell. Biochem.*, **92**, 993—1003 (2004).
27) Kingsbury M. A., Rehen S. K., Ye X., Chun J., *J. Cell. Biochem.*, **92**, 1004—1012 (2004).
28) Renbäck K., Inoue M., Ueda H., *Neurosci. Lett.*, **270**, 59—61 (1999).
29) Renbäck K., Inoue M., Yoshida A., Nyberg F., Ueda H., *Brain Res. Mol. Brain Res.*, **75**, 350—354 (2000).
30) Inoue M., Rashid M. H., Fujita R., Contos J. J., Chun J., Ueda H., *Nat. Med.*, **10**, 712—718 (2004).
31) Fujita R., Kiguchi N., Ueda H., *Neurochem. Int.*, **50**, 351—355 (2007).
32) Inoue M., Xie W., Matsushita Y., Chun J., Aoki J., Ueda H., *Neuroscience*, **152**, 296—298 (2008).
33) Ma L., Matsumoto M., Xie W., Inoue M., Ueda H., *J. Neurochem.*, **109**, 603—610 (2009).
34) Ma L., Uchida H., Nagai J., Inoue M., Chun J., Aoki J., Ueda H., *Mol. Pain*, **5**, 1—9 (2009).
35) Nagai J., Uchida H., Matsushita Y., Yano R., Ueda M., Niwa M., Aoki J., Chun J., Ueda H., *Mol. Pain*, **6**, 1—11 (2010).
36) Uchida H., Matsumoto M., Ueda H., *Neurochem. Int.*, **54**, 215—221 (2009).
37) Xie W., Uchida H., Nagai J., Ueda M., Chun J., Ueda H., *J. Neurochem.*, **113**, 1002—1011 (2010).
38) Dooley D. J., Taylor C. P., Donevan S., Feltner D., *Trends Pharmacol. Sci.*, **28**, 75—82 (2007).
39) Wu L. J., Zhuo M., *Neurotherapeutics*, **6**, 693—702 (2009).
40) Dalva M. B., Takasu M. A., Lin M. Z., Shamah S. M., Hu L., Gale N. W., Greenberg M. E., *Cell*, **103**, 945—956 (2000).

41) Kayser M. S., McClelland A. C., Hughes E. G., Dalva M. B., *J. Neurosci.*, **26**, 12152—12164 (2006).
42) Zhao J., Yuan G., Cendan C. M., Nassar M. A., Lagerström M. C., Kullander K., Gavazzi I., Wood J. N., *Mol. Pain*, **6**, 1—13 (2010).
43) Malmberg A. B., Chen C., Tonegawa S., Basbaum A. I., *Science*, **278**, 279—283 (1997).
44) Pentland B., Donald S. M., *Pain*, **59**, 159—164 (1994).
45) Osterberg A., Boivie J., Thuomas K. A., *Eur. J. Pain*, **9**, 531—542 (2005).
46) Black J. A., Renganathan M., Waxman S. G., *Brain Res. Mol. Brain Res.*, **105**, 19—28 (2002).
47) Ueda H., *Clin. Lipidol.*, **6**, 147—158 (2011).
48) Parkinson D. B., Bhaskaran A., Arthur-Farraj P., Noon L. A., Woodhoo A., Lloyd A. C., Feltri M. L., Wrabetz L., Behrens A., Mirsky R., Jessen K. R., *J. Cell Biol.*, **181**, 625—637 (2008).
49) Jessen K. R., Mirsky R., *Glia*, **56**, 1552—1565 (2008).
50) Marinissen M. J., Chiariello M., Tanos T., Bernard O., Narumiya S., Gutkind J. S., *Mol. Cell*, **14**, 29—41 (2004).
51) Barber S. C., Mellor H., Gampel A., Scolding N. J., *Eur. J. Neurosci.*, **19**, 3142—3150 (2004).
52) Fukushima N., Kimura Y., Chun J., *Proc. Natl. Acad. Sci. U.S.A.*, **95**, 6151—6156 (1998).
53) Rosen L. B., Ginty D. D., Weber M. J., Greenberg M. E., *Neuron*, **12**, 1207—1221 (1994).
54) Dai Y., Iwata K., Fukuoka T., Kondo E., Tokunaga A., Yamanaka H., Tachibana T., Liu Y., Noguchi K., *J. Neurosci.*, **22**, 7737—7745 (2002).
55) Ji R. R., Baba H., Brenner G. J., Woolf C. J., *Nat. Neurosci.*, **2**, 1114—1119 (1999).
56) Matsumoto M., Xie W., Ma L., Ueda H., *Mol. Pain*, **4**, 1—12 (2008).
57) Xie W., Matsumoto M., Chun J., Ueda H., *Mol. Pain*, **4**, 1—4 (2008).
58) Inoue M., Ma L., Aoki J., Ueda H., *J. Neurochem.*, **107**, 1556—1565 (2008).
59) Milligan E. D., Watkins L. R., *Nat. Rev. Neurosci.*, **10**, 23—36 (2009).
60) Scholz J., Woolf C. J., *Nat. Neurosci.*, **10**, 1361—1368 (2007).
61) Fujita R., Ma Y., Ueda H., *J. Neurochem.*, **107**, 152—160 (2008).
62) Ma L., Nagai J., Ueda H., *J. Neurochem.*, **115**, 643—653 (2010).

Kakiuchi et al. Molecular Pain 2011, 7:33
http://www.molecularpain.com/content/7/1/33

MOLECULAR PAIN

RESEARCH Open Access

Antinociceptive effect of cyclic phosphatidic acid and its derivative on animal models of acute and chronic pain

Yasutaka Kakiuchi[1†], Jun Nagai[2†], Mari Gotoh[1], Harumi Hotta[3], Hiromu Murofushi[1], Tomoyo Ogawa[2], Hiroshi Ueda[2] and Kimiko Murakami-Murofushi[1*]

1. Abstract

Background: Cyclic phosphatidic acid (cPA) is a structural analog of lysophosphatidic acid (LPA), but possesses different biological functions, such as the inhibition of autotaxin (ATX), an LPA-synthesizing enzyme. As LPA is a signaling molecule involved in nociception in the peripheral and central systems, cPA is expected to possess analgesic activity. We characterized the effects of cPA and 2-carba-cPA (2ccPA), a chemically stable cPA analog, on acute and chronic pain.

Results: (1) The systemic injection of 2ccPA significantly inhibited somato-cardiac and somato-somatic C-reflexes but not the corresponding A-reflexes in anesthetized rats. (2) 2ccPA reduced sensitivity measured as the paw withdrawal response to electrical stimulation applied to the hind paws of mice through the C-fiber, but not Aδ or Aβ. (3) In mice, pretreatment with 2ccPA dose-dependently inhibited the second phase of formalin-induced licking and biting responses. (4) In mice, pretreatment and repeated post-treatments with 2ccPA significantly attenuated thermal hyperalgesia and mechanical allodynia following partial ligation of the sciatic nerve. (5) In rats, repeated post-treatments with 2ccPA also significantly attenuated thermal hyperalgesia and mechanical allodynia following chronic sciatic nerve constriction.

Conclusions: Our results suggest that cPA and its stable analog 2ccPA inhibit chronic and acute inflammation-induced C-fiber stimulation, and that the central effects of 2ccPA following repeated treatments attenuate neuropathic pain.

2. Background

Cyclic phosphatidic acid (cPA) was originally isolated from myxoamoebae of a true slime mold, *Physarum polycephalum*, in 1992 [1]. The chemical formula of cPA is similar to that of lysophosphatidic acid (LPA), but cPA has a unique structure with a cyclic phosphate ring at *sn*-2 and *sn*-3 of the glycerol backbone [2]. These features provide cPA with distinct/opposing biological functions from those of LPA. For instance, LPA stimulates cell proliferation and cancer cell invasion, while cPA inhibits these activities [3-8]. Interestingly, LPA is enzymatically generated from transphosphatidylation of lysophosphatidylcholine by autotaxin (ATX) [9], but cPA inhibits ATX activity [10]. Thus, cPA could be an endogenous inhibitor of LPA production through ATX.

Exogenous and endogenous LPA cause acute pain through C-fibers and neuropathic pain [11-13]. Recent studies revealed that nerve injury-induced LPA production and neuropathic pain were significantly attenuated in mice with heterozygous ATX deficiency [14,15]. In this study, we characterized the effects of cPA and its chemically stable analog 2ccPA on acute and neuropathic pain.

3. Methods

3.1. Recording the somato-cardiac sympathetic reflex

The experiments were performed using male Wistar rats (n = 11) weighing 270-370 g anesthetized by

* Correspondence: murofushi.kimiko@ocha.ac.jp
† Contributed equally
[1]Department of Biology, Faculty of Science, Ochanomizu University, 2-1-1 Ohtsuka, Bunkyo-ku, Tokyo 112-8610, Japan
Full list of author information is available at the end of the article

intraperitoneal (i.p.) application of urethane (1.1 g/kg). A femoral vein was catheterized for intravenous (i.v.) administration of supplemental anesthetics and cPA. A femoral artery was catheterized to record arterial blood pressure and heart rate. The animals were immobilized by gallamine triethiodide (20 mg/kg i.v. as required) and artificially ventilated via tracheal cannula. Ventilation was monitored with a gas analyzer (1H26; NEC San-ei, Tokyo) and adjusted to maintain an end-tidal CO_2 level of 3.0%. Body temperature was maintained at 37.5°C using an automatically regulated heating pad and lamp (ATB-1100; Nihon Kohden, Tokyo). Both vagal nerves were cut at the cervical level to prevent vagal contamination of the recorded sympathetic nerve activity.

With the rat placed in the supine position, the right second costal bone was removed. The right inferior cardiac sympathetic nerve was dissected retropleurally, cut as close to the heart as possible, and covered with warm paraffin oil. Cardiac sympathetic efferent nerve activity was recorded from the central segment of the cardiac sympathetic nerve with platinum-iridium wire electrodes using an AC preamplifier (S-0476; Nihon Kohden, Tokyo; time constant set at 0.33 s). Reflex responses elicited by electrical stimulation of a hind limb nerve were averaged (50 trials) by a computer (ATAC 3700; Nihon Kohden, Tokyo or UPO, Unique Medical, Tokyo). The averaged responses were stored as digital signals and recorded on a printer or mini-writer. The size of the reflex response was measured as the area under the evoked response and expressed as the percent of the control size preceding drug injection.

A tibial nerve was dissected from the surrounding tissues and cut. The central cut end segment of the nerve was placed on bipolar platinum-iridium wire electrodes for electrical stimulation. Single square pulse stimuli of 0.5 ms duration were delivered every 3 s by a digital electrical stimulator (SEN-7103; Nihon Kohden, Tokyo).

3.2. Recording spinal somato-somatic reflex

Male Wistar rats (n = 4; weighing 330-350 g) were anesthetized using pentobarbital (50 mg/kg i.p.). A jugular vein was catheterized for i.v. administration of cPA. Body temperature was maintained at 37.5°C. The spinal cord was completely transected at the upper thoracic level.

With the rat placed in the supine position, a branch of the right saphenous nerve innervating thigh skin was cut at the thigh level. The central cut end segment of the nerve was stimulated electrically as described above. Electromyogram (EMG) was recorded from the right leg muscles by inserting silver electrodes using the AC preamplifier. With single shocks, post-stimulus time histograms were created by a computer (ATAC 3700; Nihon Kohden, Tokyo) for EMG activity for approximately 50 trials at 3-s intervals. The averaged responses were stored as digital signals and recorded on a mini-writer. The size of the reflex response was measured as the area under the evoked response and expressed as the percent of the control size preceding drug injection.

3.3. Electrical stimulation-induced paw withdrawal (EPW) Test

Male C57BL/6 mice (TEXAM, Japan) weighing 18-22 g were used. The electrical stimulation-induced paw withdrawal (EPW) test conducted using the Neurometer™ CPT/C (Neurotron Inc.) has been reported previously [16]. In brief, electrodes were fastened to the plantar surface and instep of the mice. Transcutaneous nerve stimuli with each of the 3 sine wave pulses (5, 250, and 2000 Hz) were applied using the Neurometer™. The minimum intensity at which each mouse exhibited paw withdrawal was defined as the current stimulus threshold at 10-15 min after i.v. 2ccPA injection.

3.4. Formalin test

According to several preceding works [17,18] and to an economical advantage, we used ICR (CD1) female mice (Charles River, Japan), 6-9 weeks of age for the formalin test. Formalin solution (30 μL, 2% v/v) in saline was subcutaneously (s.c.) injected into the plantar surface of the left hind paw. Immediately after the formalin injection, the animals were placed in a cage and videotaped for 30 min from beneath the transparent floor. The time (in seconds) spent licking and biting the injected paw was counted in 5-min intervals by videotape observation. Two distinct phases of intensive licking and biting activities identified as the early and late phases were defined at 0-10 min and 10-30 min, respectively. At 3 min before formalin was injected, 2ccPA solution (in PBS containing 1% BSA) was i.v. injected. Morphine hydrochloride solution (Takeda Pharmaceutical Company, Osaka, Japan) in saline was i.p. injected at 30 min before formalin injection.

3.5. Neuropathic pain models

In experiments using the C57BL/6 mice, partial ligation of the sciatic nerve was performed under pentobarbital (50 mg/kg) anesthesia, following the methods of Malmberg and Basbaum [19]. 2ccPA was dissolved in artificial cerebrospinal fluid (aCSF: 125 mM NaCl, 3.8 mM KCl, 1.2 mM KH_2PO_4, 26 mM $NaHCO_3$, 10 mM glucose, pH 7.4). The intrathecal injection (i.t.) of 2ccPA was given into the space between spinal L5 and L6 segments according to the method of Hylden and Wilcox [20]. In the thermal paw withdrawal tests, nociception was measured as the latency to paw withdrawal evoked by exposure to a thermal stimulus [21,22]. Unanesthetized animals were placed in Plexiglas cages on the top of a glass sheet and were allowed an adaptation period of 1

h. A thermal stimulator (IITC Inc., Woodland Hills, CA, USA) was positioned under the glass sheet, and the focus of the projection bulb was aimed precisely at the middle of the plantar surface of the animal. A mirror attached to the stimulator permitted plantar surface visualization. The paw pressure test was performed, as described previously [22]. Mice were placed into a Plexiglas chamber on a 6 × 6 mm wire-mesh grid floor and allowed to acclimatize for 1 h. A mechanical stimulus was delivered onto the middle of the plantar surface of the right hind paw using a Transducer Indicator (Model 1601; IITC Inc., Woodland Hills, CA, USA). The pressure needed to induce a flexor response was defined as the pain threshold.

In experiments using rats, the chronic constriction injury was produced according to the procedure of Bennett and Xie [23]. Briefly, rats (182-216 g at day of ligation) were anesthetized with sodium pentobarbital (Nembutal, Dainippon pharmaceutical co., 40 mg/kg i.p.). The left sciatic nerve was exposed at mid-thigh level. Three loose ligatures with 4.0 chromic gut (SG-535; Syneture, USA), about 1-mm spacing, were tied around the sciatic nerve proximal to the trifurcation. Six days after nerve ligation, the development of neuropathy was assessed by measuring paw withdrawal latencies against thermal and mechanical stimuli [24,25]. Briefly, the thermal withdrawal threshold of a hind paw was measured using a beam of radiant infrared heat and a photocell (Planter Test model 7370; Ugo Basil, Milan, Italy). To prevent tissue damage, the cut-off time was set to 20 or 30 sec for rats with or without ligation. The mechanical withdrawal threshold was measured by the von Frey filament test. All rats were administered drug treatment by i.v. injection, and experiments were performed at 10 min and at 2 and 4 hours after drug treatments.

3.6. Drugs

We used chemically synthesized cPA 18:1 and its biologically stable derivative, 2-carba cPA 16:1 (2ccPA) (Figures 1A, B) [6]. These compounds were i.v. or i.t administered after they were dissolved in saline or artificial cerebrospinal fluid (aCSF).

3.7. Statistical analysis

Data were expressed as mean ± S.E. The data were statistically analyzed by Student's t-test, Welch's test, Steel's test, Dunnett's test, Wilcoxon test, or Tukey's multiple comparison tests. A P value < 0.05 was considered statistically significant.

3.8. Ethical approval

All the experiments were performed with an approval of the Animal Care and Use Committee at the Tokyo Metropolitan Institute of Gerontology and Nagasaki University Animal Care Committee at the Nagasaki University Graduate School of Biomedical Sciences (reference number 0706130596).

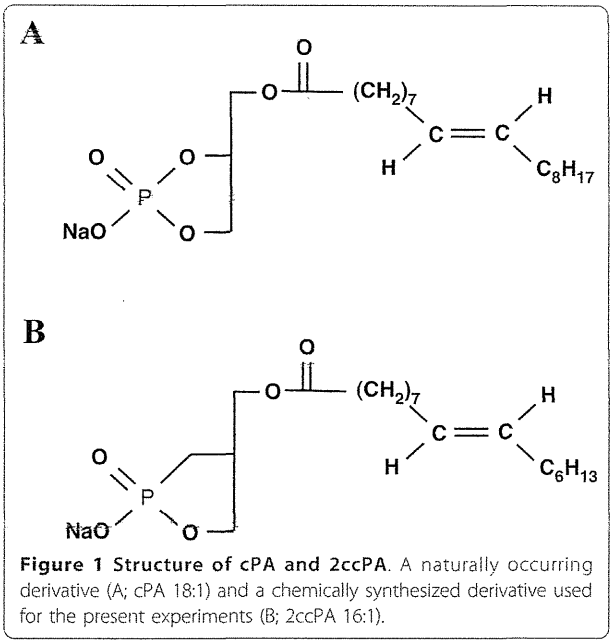

Figure 1 Structure of cPA and 2ccPA. A naturally occurring derivative (A; cPA 18:1) and a chemically synthesized derivative used for the present experiments (B; 2ccPA 16:1).

4. Results

4.1. Effects of cPA and 2ccPA on somato-cardiac sympathetic A- and C-reflexes in anesthetized rats

Single shock stimulation of A- and C-afferent fibers of the tibial nerve (at 10 V with 0.5 ms pulse duration) elicited 2 types of cardiac sympathetic reflex discharges as shown in Figure 2A. These discharges occur in a short latency (about 40 ms) as the A-sympathetic reflex and in a long latency (about 210 ms) as the C-sympathetic reflex, respectively (Figure 2A).

Intravenous injection of 0.1 mg/kg of 2ccPA depressed the C-reflex but not the A-reflex (Figure 2A). In most experiments, the 2ccPA-induced depression of C-reflex components started several minutes after the injection, reached its maximum level in less than 15 min, and then gradually returned to baseline within 40 min. The response was reproducible in successive trials on the same animal. Injection of 2ccPA 18:1 also yielded similar C-reflex suppression (data not shown).

Figure 2B summarizes the effects of i.v. injection of 2ccPA and cPA on the C-reflex in 8 rats. The responses were measured at 10-15 min after i.v. injection of cPA, i.e., after reaching the maximum effect (see above). After injection of 0.2 mg/kg 2ccPA, the C-reflex reached 82 ± 9% of the control. Injection of 2 mg/kg, but not 0.2 mg/kg cPA, significantly depressed the C-reflex.

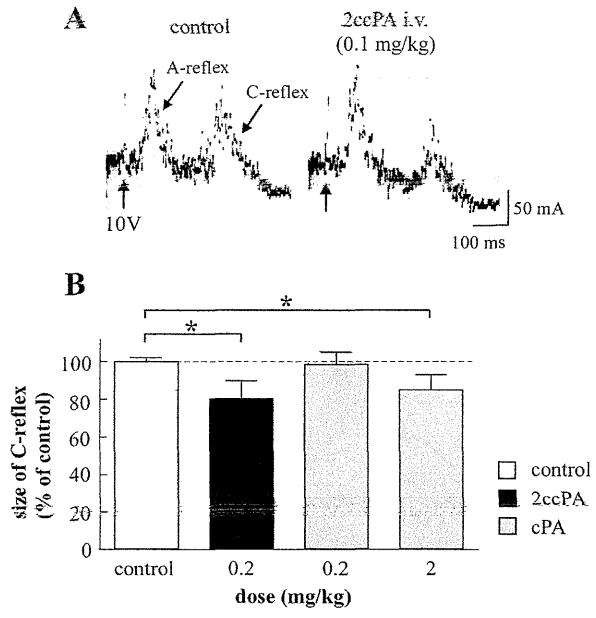

Figure 2 Effects of i.v. cPA and 2ccPA on somato-cardiac sympathetic A- and C-reflexes. A, Specimen records of A- and C-reflexes (averages of 50 trials) elicited by single electrical stimulation of a tibial nerve using 10 V of stimulus strength. Left: prior to 2ccPA application (control). Right: 15 min after i.v. injection of 0.1 mg/kg 2ccPA. B, Graphical summary of the size of the C-reflex at 0-5 min before cPA/2ccPA injection (control; n = 8), at 10-15 min after i.v. injection of 0.2 mg/kg 2ccPA (n = 4), and 0.2 mg/kg (n = 4) and 2 mg/kg (n = 4) cPA. We averaged 1-2 trials for each rat. The mean size (area under the evoked response curve) of the C-reflex at 0-10 min before each injection was expressed as 100%. All subsequent reflexes were expressed as percentages of the control values. Each column and vertical bar represent mean and S.E. *P < 0.05; significantly different from the control response by Student's t-test.

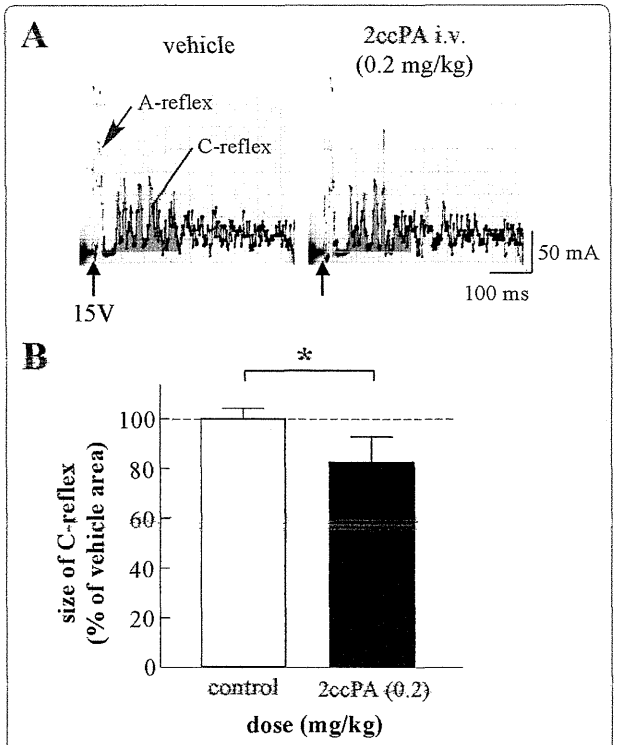

Figure 3 Effects of i.v. 2ccPA on the somato-somatic C-reflex. A, Specimen records of A- and C-reflexes (averages of 50 trials) elicited by single electrical stimulation of a saphenous nerve using 15 V of stimulus strength. Left: prior to 2ccPA application (control). Right: 10 min after i.v. injection of 0.2 mg/kg 2ccPA.B, Graphical summary of the size of the C-reflex at 0-5 min before 2ccPA injection (control; n = 4) and at 10-15 min after i.v. injections of 0.2 mg/kg 2ccPA (n = 4). We averaged 1-2 trials for each rat. The mean size (area under the evoked response curve) of the C-reflex at 0-10 min before each injection was expressed as 100%. All subsequent reflexes were expressed as percentages of the control values. Each column and vertical bar represent mean and S.E. *P < 0.05; significantly different from the control response by Student's t-test.

After injection of 2 mg/kg cPA, the C-reflex reached 86 ± 8% of the control.

4.2. Effects of cPA and 2ccPA on somato-somatic A- and C-reflexes in anesthetized rats

The hypothesis that cPA acts at the primary afferent nerve terminals was tested by recording spinal somato-somatic reflexes in 4 rats (Figure 3). Stimulation of the myelinated A-afferent fibers and unmyelinated C-afferent fibers of the saphenous nerve (at 15 V with 0.5 ms pulse duration) produced 2 distinct A- and C-somatic reflex components in the hind limb EMG, i.e., a short latent (about 10 ms) A-reflex and long latent (about 70 ms) C-reflex. Intravenous application of the same 2ccPA dose (0.2 mg/kg) that depressed the somato-sympathetic C-reflex also depressed the C-somatic reflex component to a similar magnitude. After injection of 0.2 mg/kg 2ccPA, the C-reflex reached 83 ± 5% (n = 4) of the control ($p < 0.05$).

4.3. C-fiber specific analgesic effects of 2ccPA on electrical stimulation-induced paw withdrawal (EPW)

We established the EPW test to distinguish responses mediated by different sensory fibers [16]. The hind paw is given transcutaneous nerve stimuli with sine-wave pulses of 5, 250, or 2000 Hz to stimulate C-, Aδ-, or Aβ-fibers [26,27], and the intensity (μA) required to induce a withdrawal reflex was defined as the threshold. The thresholds of naïve mice for 5, 250, and 2000 Hz stimuli were 64.4 ± 1.9 (C-fibers), 145.0 ± 4.5 (Aδ-fibers), and 401.1 ± 13.6 (Aβ-fibers). When the EPW test was performed at 10-15 min after the 2ccPA (i.v.) injection, the threshold increased in a dose-dependent manner with 5 Hz, but it did not increase with 250- or 2000-Hz stimuli (Figure 4).